Spring 5-1-2021

"Climatic Controls of Plant Productivity, Phenology, and Physiology in Drylands

Alesia Hallmark
University of New Mexico

Scott L. Collins
University of New Mexico - Main Campus

Marcy E. Litvak
University of New Mexico - Main Campus

Christopher D. Lippitt
University of New Mexico - Main Campus

Andrew D. Richardson
Northern Arizona University

Alesia Jane Hallmark
Candidate

Biology Department
Department

This dissertation is approved, and it is acceptable in quality and form for publication:

Approved by the Dissertation Committee:

Dr. Scott L. Collins, Chairperson

Dr. Marcy E. Litvak, Chairperson

Dr. Chris D. Lippitt

Dr. Andrew D. Richardson

CLIMATIC CONTROLS OF PLANT PRODUCTIVITY, PHENOLOGY, AND PHYSIOLOGY IN DRYLANDS

by

ALESIA JANE HALLMARK

B.S., Zoology, Oklahoma State University, 2011
B.S., Botany, Oklahoma State University, 2011
M.S., Biology, University of New Mexico, 2016

DISSERTATION

Submitted in Partial Fulfillment of the
Requirements for the Degree of

Doctor of Philosophy
Biology

The University of New Mexico
Albuquerque, New Mexico

May, 2021

DEDICATION

This work is dedicated to my grandmothers, Bonnie Hallmark, Linda Berry, and Mary Whitener. Without their strength and caring, I would not be me.

ACKNOWLEDGMENTS

I would like to first acknowledge my dissertation chairpersons, Dr. Scott Collins and Dr. Marcy Litvak. Thank you for welcoming me into your labs, guiding me throughout my time as a graduate student, providing me with mentoring opportunities and teaching me everything from how to successfully collaborate to how to dig soil pits and solder wires. Thank you to my committee members, Dr. Chris Lippitt, Dr. Andrew Richardson, and Dr. Jenn Rudgers for the kind and enthusiastic support.

Thank you to Sevilleta National Wildlife Refuge and U.S. Fish & Wildlife staff, especially Kathy Granillo and Jon Erz, for allowing me to conduct so much exciting research on the Refuge. Thank you to the Sevilleta Long-Term Ecological Research program, and Dr. Jennifer Rudgers in particular, for providing so much of the data used in my dissertation, multiple years of financial support, and an exciting research community. Thank you to all of the field crew and staff members that collected the data I used.

Thank you to my labmates, especially Tim Ohlert, Dr. Amy Bennett, Dr. Greg Maurer, Dr. Rob Pangle, Diana Macias, Dr. Jen Noble, Dr. Syd Jones, and Juan Camacho, for the many hours of conversation around the whiteboard. Thank you also to my best friends Wyatt Sharber and Aneliese Apala-Flaherty for supporting me in life and in scientific endeavors since high school. Thank you to Gregor Hamilton for…everything.

This research was supported by grants from the National Science Foundation to the University of New Mexico for Long-term Ecological Research including DEB #1748133 and #1655499 and from the Ameriflux Management Project, Department of Energy Subcontract Number 7074628.

CLIMATIC CONTROLS OF PLANT PRODUCTIVITY, PHENOLOGY, AND PHYSIOLOGY IN DRYLANDS

by

Alesia Jane Hallmark

B.S., Zoology, Oklahoma State University, 2011
B.S., Botany, Oklahoma State University, 2011
M.S., Biology, University of New Mexico, 2016
Ph.D. Biology, University of New Mexico, 2021

ABSTRACT

Drylands play a critical role in global carbon dynamics. Anthropogenic climate change is causing these hot and dry regions to become increasingly hotter, drier, and more variable. This is especially concerning as drylands are some of the most sensitive regions to changes in aridity. It is critical to understand how dryland plant species might react to a changing climate. In this dissertation, I explored the relative effects of plant community composition and dominant species abundance on determining ecosystem-wide carbon dynamics. I compared the population stability of 98 dryland plant species and related stability to phenological traits. Lastly, I related branch movements of a common desert shrub to a number of micrometeorological measurements. This dissertation contributes to scientific understanding of dryland plant species, how and when they contribute to carbon cycling, balance growth and reproductive investment, and leverage physiological traits to survive in dry and variable abiotic conditions.

TABLE OF CONTENTS

List of Figures

List of Tables

Chapter 1

Introduction

Carbon uptake in drylands is a globally important process. Drylands are widespread, covering ~45% of the Earth's terrestrial surface (Taylor and Lloyd 1992, Lal 2003, Huang et al. 2015). Even though drylands are less productive than more mesic regions, they have a large collective carbon sink and over ~40% of humans rely on food harvested from drylands (Reynolds et al. 2007). Drier biomes are more sensitive to interannual variation in rainfall, resulting in large fluctuations in primary productivity between wet and dry years (Rudgers et al. 2018, Maurer et al. 2020). The variability of dryland carbon uptake explains a large portion of the variation in the global land carbon sink (Ahlström et al. 2015). Because drylands are so important to human life and global carbon cycling, it is of great concern that drylands are becoming more arid and more variable at a faster rate than neighboring mesic biomes (Gutzler and Robbins 2010, Maurer et al. 2020). Aridification, in addition to increased land use pressures, is expanding the extent of drylands (Burrell et al. 2020).

In drylands, plant growth occurs in pulses following stochastic precipitation events (Beatley 1974, Peñuelas et al. 2004, Crimmins et al. 2011). Species that live in these extreme, unpredictable conditions have developed an array of adaptive strategies to take advantage of limited resources when they come available or to survive the intervening drought conditions. Some species have acquisitive growth strategies, growing and reproducing quickly in wet seasons or years. The synchronized "boom" of these

populations results in increased species richness and diversity, potentially creating surges of ecosystem services (Chesson et al. 2004). Other species remain abundant throughout dry and wet periods. These common species may have physical traits (i.e. deeper roots or waxy cuticles) or physiological strategies (i.e. C_4 or CAM photosynthesis or diel activity patterns) that allow them to weather unfavorable conditions.

In Chapter 2, I explored the relative effects of plant community diversity versus evenness on determining ecosystem-wide carbon dynamics. While more species-rich, diverse plant communities are more productive in some ecosystems (*diversity-functioning hypothesis*), productivity in other biomes is more strongly influenced by the abundance of one or a few dominant species (*mass-ratio hypothesis*). Most studies exploring these relationships have taken place in mesic grasslands. I explored the influence of these two hypotheses in two dryland biomes: a desert grassland dominated by black grama grass (*Bouteloua eriopoda*) and a creosote shrubland dominated by creosote bush (*Larrea tridentata*), both located within Sevilleta National Wildlife Refuge in central New Mexico, USA. At each of these sites, I paired ten years of eddy covariance carbon flux data with biannual plant community surveys and PhenoCam-derived vegetation indices. If the diversity-functioning hypothesis was supported in these biomes, I expected ecosystem carbon fluxes to be more strongly related to plant species richness and community diversity. I also expected the productivity of the whole plant community to best predict ecosystem carbon fluxes on seasonal time steps and the phenological activity of the whole plant community to best predict ecosystem carbon fluxes on daily time steps. Alternatively, if the mass-ratio hypothesis was supported, I expected community evenness to be a strong negative predictor of ecosystem carbon. Likewise, I also expected the abundance of the

dominant species alone to best predict ecosystem carbon fluxes on seasonal time steps and the vegetative phenology of the dominant species to best predict ecosystem carbon fluxes on daily time steps, at least in some seasons.

The temporal stability of plant populations, whether they fluctuate or remain steady from year to year, has been associated with vegetative growth such as leaf dry matter content (Májeková et al. 2014). However, few studies have related population stability to phenological traits, which can be used to quantify both the vegetative and reproductive strategies of species. In Chapter 3, I compared the population stability of 98 dryland species to their vegetative and reproductive phenological traits. growing across the desert grassland, creosote shrubland, and Great Plains grassland biomes of Sevilleta National Wildlife Refuge. I paired 18 years of biannual biomass estimates, monthly phenological observations, and monthly precipitation and air temperature data. From these, I quantified population variability over time, the onset and offset dates of vegetative and reproductive phenophases, the duration of phenophases, and associated climatic factors. I predicted that species with longer vegetative phenophases would be adapted to living through a larger range of temperatures and water availability, and therefore would have more stable population sizes over time. However, I did not know how these characteristics would relate to reproductive traits such as the timing and duration of reproduction or reproductive success.

Finally, in Chapter 4, I focused on a widespread and important species of North American deserts, creosote bush (*Larrea tridentata*). Using photographs taken at hourly intervals over the course of >4 months (July-December), I tracked the periodic movements of live and dead branches. I related branch movements to a number of abiotic factors and

predicted that movements would be most strongly related to water pressure within stems or the atmospheric water demand. I also explored potential plant-environmental feedbacks between branch movements and soil temperatures. In addition to my in-depth look at creosote bush, I also surveyed time-lapse imagery from around the country and documented woody branch movements, a rarely described phenomenon, at over 50 sites across the United States.

With these chapters, I hoped to contribute to our scientific understanding of dryland plant species, how and when they contribute to carbon cycling, their strategies for balancing growth and reproductive investment, and physiological traits they may have developed to survive in dry and variable abiotic conditions.

All chapters are either already submitted or being prepared for publication in peer-reviewed journals.

Chapter 2

Dominant species regulate ecosystem carbon fluxes in two semi-arid systems

Authors: Alesia J. Hallmark[1], Scott L. Collins[1], Jennifer A. Rudgers[1], Marcy E. Litvak[1]

[1] Department of Biology, University of New Mexico, Albuquerque, NM, USA

2.1 Introduction

The productivity of drylands is a critical component of global carbon cycling. Drylands cover a large portion (~45%) of the Earth's terrestrial surface (Taylor and Lloyd 1992, Lal 2003, Huang et al. 2015) and house ~40% of the human population (Reynolds et al. 2007). The extent of drylands is expanding due to land use practices and anthropogenic aridification (Burrell et al. 2020). Although productivity in drylands is low, the collective carbon sink is large and regulates the interannual variation and trend in the global land carbon sink (Ahlström et al. 2015). In drylands, stochastic precipitation events drive variability in plant growth (Beatley 1974, Peñuelas et al. 2004, Crimmins et al. 2011). Changes in ecosystem function are often attributable to climate-driven changes in the underlying plant community structure (Grime et al. 2000, Kahmen et al. 2005, Avolio et al. 2014). This is a concern because drylands, in particular, are highly sensitive to warming and increased climate variability (Maurer et al. 2020), both of which are predicted to increase in the coming century (Gutzler and Robbins 2010, Rudgers et al. 2018). A more

complete understanding of the specific changes in community structure that impact ecosystem scale photosynthesis and ecosystem respiration will increase our understanding of the mechanisms driving interannual variability of carbon sequestration in these biomes and our ability to predict how these processes will change in the coming decades.

The variable community structure and dynamic plant growth patterns of drylands make them excellent natural systems in which to explore how plant community structure and individual species might affect ecosystem carbon fluxes. Stochastic precipitation events cause many pulses of plant growth within a year because water is the most limiting resource in drylands (Noy-Meir 1973). Each of these pulses can promote a different cohort of plant species with differing carbon uptake dynamics (Venable and Kimball 2012, Fu et al. 2017, Silva et al. 2017). The onset and duration of growth differ based on rooting depth, water storage ability, germination strategies, and previous growth (Beatley 1974, Crimmins et al. 2010, Ogle et al. 2015). In drylands, annual species can also account for a significant, if ephemeral, portion of the plant community (Guo and Brown 1996, Chesson et al. 2004). Pulses of perennial plant growth and annual plant recruitment produce large intra- and inter-annual variability in community structure (Collins et al. 2014, Ahlström et al. 2015). Linking pulses of individual species, and the climate factors that regulate them with ecosystem fluxes would greatly increase our understanding of intra- and inter-annual variability in carbon fluxes in these biomes.

Multiple facets of plant community structure have been linked to ecosystem functioning. A number of studies have found that species richness and diversity are positively correlated with productivity, (*the diversity-ecosystem function hypothesis*) although the generality and the underlying mechanisms are debated, and the strongest

evidence has come from diversity experiments in mesic grasslands (Hector et al. 1999, Tilman et al. 2001, Hooper et al. 2016). In drylands, higher species richness, though not the sole driver, is often associated with increased ecosystem functioning (Maestre et al. 2012). Subordinate or even rare species can contribute to ecosystem functioning when more common species decline in abundance or resources become more abundant (Collins et al. 1998, Lyons and Schwartz 2001, Smith and Knapp 2003, Cardinale et al. 2011). A competing paradigm (*the mass ratio hypothesis*) argues that the productivity of one or a few dominant (abundant and common) species explains most of the variation in community productivity (Whittaker 1965, Grime 1998, Avolio et al. 2019). This hypothesis has been supported in a number of experimental studies where ecosystem functions such as productivity, stability, and invasibility were correlated with dominant species abundance or degree of dominance (Smith and Knapp 2003, Mulder et al. 2004, Emery and Gross 2007). Dominant species in natural systems can maintain or even increase functioning when species richness decreases (Winfree et al. 2015, Hillebrand et al. 2018, Su et al. 2019, Sonkoly et al. 2019). The phenology of individual species may lead them to contribute differentially to carbon dynamics throughout a year. Disentangling the importance of these two competing hypotheses at the ecosystem scale can expand our understanding of diversity-productivity relationships in dryland biomes.

Few studies have combined explicit measures of community structure with ecosystem-scale fluxes to study how diversity and dominance affect ecosystem functioning (but see Hirota et al. 2010, Wang et al. 2016, Sagar et al. 2019). Eddy covariance technology continuously measures ecosystem-scale carbon fluxes between the atmosphere and biosphere (Baldocchi et al. 2001, Novick et al. 2018), integrating the activities of all

organisms within the ecosystem, as well as the abiotic conditions in which they occur (Catovsky et al. 2002, de Bello et al. 2010). Previous studies have found that carbon fixation is sensitive to differences in species composition and structure within the tower fetch (Boeck et al. 2007, Monson et al. 2010, Laganière et al. 2015, Rutledge et al. 2017, Duman and Schäfer 2018). In most tower sites, plant abundance and composition are only directly measured once per growing season, limiting the ability to link plant community structure to ecosystem functioning. Although this relationship may vary on shorter time scales, especially in pulse-driven drylands, it is not feasible to manually monitor community structure at the spatial scale or temporal frequency required to match eddy covariance technology.

Digital repeat photography bridges the gap between sensor measurements of carbon fluxes and manual observations of plants by producing automated photographs of landscapes, canopies, or particular plant species using low-cost, commercially available cameras. Both the timing and magnitude of vegetative phenology of plants can be quantified using vegetation indices (VI's) derived from time series of these digital photographs. The relationship between VI's and ecosystem carbon uptake is well-documented (Migliavacca et al. 2011, Hufkens et al. 2012, Toomey et al. 2015), even in drylands where heterogenous vegetation and highly stochastic growth makes plant productivity difficult to capture with manual measurements (Yan et al. 2019). Research networks, such as the PhenoCam Network in North America are co-locating cameras with flux towers, standardizing methodology across sites, and making time series of vegetation indices freely available for public use (Seyednasrollah et al. 2019). Most previous studies that have related VI's to carbon fluxes have done so at the community scale, averaging the

vegetative phenology of every species in a given landscape. However, individual plant species can be differentiated in camera images, enabling the detection of plant species-specific phenology, especially that of the dominant species within each scene. This bridge from "species-blind" sensor measurements to direct observations of growth can be used to link the phenological activity of common species to high-frequency ecosystem-scale flux, and identify potential abiotic drivers (temperature, water availability, or light availability) of species growth. Incorporating finer resolution metrics of growth can verify if daily carbon fluxes are more related to the vegetative phenology of dominant species or a suite of species within the community, and if these relationships vary throughout the year (Huang et al. 2019).

Here, we linked measurements of ecosystem carbon fluxes, plant community composition, and digital repeat photography from two flux towers located in distinct semi-arid biomes in central New Mexico, USA. While the climates of these biomes are similar, plant community composition differs, enabling tests of the degree to which individual plant species versus whole communities influence ecosystem processes in these biomes. Using this ecological monitoring network, we sought to answer the central question: Which is a better predictor of ecosystem carbon fluxes: the diversity of the plant community (diversity-ecosystem functioning hypothesis) or the abundance of dominant plant species (mass-ratio hypothesis)? We addressed this question using the following metrics: (1) plant community composition (species richness, diversity, and dominance) and abundance (of the whole community and the dominant species) measured on seasonal time scales, as captured by traditional plant biomass estimates from boots-on-the-ground quadrats, (2) phenological activity of the full plant community and common plant species, as captured

by camera imagery, and (3) climatic variables (temperature, precipitation, sunlight) that were most associated with the phenology of common species and the whole community.

If the diversity-ecosystem functioning hypothesis predominates at a site, we predicted that ecosystem carbon fluxes will be positively correlated with species richness, diversity, and seasonal community abundance. Fluxes will be correlated with either community-average phenology or the phenology of a complementary suite of species throughout the year. And finally, the potential abiotic drivers of ecosystem carbon fluxes will be similar to those of community-average phenology. Alternatively, if the mass-ratio hypothesis predominates, we predicted that ecosystem carbon fluxes will be negatively correlated with species evenness and positively correlated with the abundance of the dominant species. Fluxes will be correlated with the phenology of the dominant species and the potential abiotic drivers of fluxes will be similar to those of the dominant species.

2.2 Methods

2.2.1 Study Sites

Data were collected at two eddy flux tower sites, one in a desert grassland and the other in a creosote shrubland, both deployed in 2007 and located within the Sevilleta National Wildlife Refuge (SNWR), in central New Mexico, USA (D'Odorico et al. 2010b, Anderson-Teixeira et al. 2011b, Petrie et al. 2014). The SNWR is located along the northern range boundary of the Chihuahuan desert. Our two study sites are located less than 5 km of one another and experience very similar climates.

The desert grassland site is a Chihuahuan Desert grassland dominated by black grama grass (*Bouteloua eriopoda*), which contributes ~73% of the aboveground biomass

at the site (Table 1). The Ameriflux designation of this site is US-Seg and it is located at 34.3623 N, -106.7019 W, at an elevation 1622 m. The next most common species are winterfat (*Krascheninnikovia lanata*), lacy tansyaster (*Machaeranthera pinnatifida*), and snakeweed (*Gutierrezia sarothrae*), all perennial forbs or subshrubs (Table 1). While these three species are present at the site in most years, they are much less abundant than black grama grass, so we classify them as subordinate species in this community. A lightning-induced wildfire burned this site in August 2009. Post-fire, the cover of grasses decreased and annual forbs increased. By the fall of 2013, the cover of black grama grass recovered to pre-fire levels. The creosote shrubland site is a Chihuahuan Desert creosote shrubland. It is dominated by creosote (*Larrea tridentata*), which contributes ~76% of the aboveground biomass at the site. The Ameriflux designation for this site is US-Ses and it is located at 34.3349 N, -106.7442 W, at an elevation 1593 m. Patches of intermixed black grama grass (*Bouteloua eriopoda*), James' galeta grass (*Pleuraphis jamesii*), and sand dropseed (*Sporobolus* spp.) as well as scattered snakeweed (*Gutierrezia sarothrae*) grow in intercanopy spaces (Table 1). In February 2011, a severe freeze event occurred across the SNWR, with temperatures dropping below -31C, 20C below the average minimum winter temperature for these sites (Ladwig et al. 2019). Although the freeze event detrimentally affected all communities, the consequences were most apparent at the shrubland site. Creosote suffered up to a 94% loss of canopy cover in some areas (Ladwig et al. 2019).

Mean annual precipitation at our study sites from the years 2010-2019 was 214.0 ± 4.9 mm at the creosote shrubland site and 231.6 ± 5.1 mm at the desert grassland site. The majority of this rain fell during the monsoon rainy season (July-October) in each year.

Mean annual temperature was 14.5 ± 0.1 C at the creosote shrubland site and 13.8 ± 0.0 at the desert grassland site. The average dry weight of aboveground biomass in the more productive monsoon rainy season was 96.6 ± 3.5 g/m^2 at the creosote shrubland site and 110.6 ± 5.7 g/m^2 at the desert grassland site. The mean average species richness (number of species comprising at least 0.05% m^2) was 17.4 ± 0.4 species at the creosote shrubland site and 12.0 ± 0.5 species at the desert grassland site.

Table 2.1. Common species at each study site. Species that are consistently the most abundant over time are denoted as dominant, while species that are very common but much less abundant are denoted as subordinate. Aboveground biomass is used as a proxy for abundance. Numeric values represent the mean ± the standard error of fall (monsoon) season surveys, 2010-2019.

Site	**Species**	**Dominance**	**Functional Group**	**Average fall mass (g/m^2)**	**Average relative abundance (%)**	**Average rank abundance**
desert grassland	*Bouteloua eriopoda*	dominant	C4 grass	78.5 ± 3.6	73 ± 1.5	1.0 ± 0.0
	Krascheninnikovia lanata	subordinate	C3 subshrub	4.6 ± 0.2	4.9 ± 0.3	3.1 ± 0.1
	Machaeranthera pinnatifida	subordinate	C3 forb	9.1 ± 1.0	8.8 ± 1.1	3.5 ± 0.2
	Gutierrezia sarothrae	subordinate	C3 subshrub	2.3 ± 0.2	2.1 ± 0.1	5.4 ± 0.2
creosote shrubland	*Larrea tridentata*	dominant	C3 shrub	73.5 ± 2.8	76.0 ± 0.6	1.0 ± 0.0
	Bouteloua eriopoda	subordinate	C4 grass	1.7 ± 0.1	1.9 ± 0.1	5.3 ± 0.3
	Pleuraphis jamesii	subordinate	C4 grass	1.5 ± 0.1	1.8 ± 0.12	6.9 ± 0.3
	Sporobolus spp.	subordinate	C4 grass	0.7 ± 0.1	0.7 ± 0.0	11.5 ± 0.5
	Gutierrezia sarothrae	subordinate	C3 subshrub	5.4 ± 0.6	5.1 ± 0.5	17.0 ± 4.0

2.2.2 Direct biomass measurements

At the desert grassland tower site, we surveyed plant species biannually in twenty 1 m^2 fixed-position plots located within 100 m of the tower. At the creosote shrubland site, we surveyed biannually in sixteen 1 m^2 fixed-position plots located within 500 m of the tower. Within each of these plots, we assessed plant abundance and biomass data using non-destructive methods. Every plant was identified to species and measured. We recorded

the ground cover (m^2) and height (cm) of each individual. We converted these measurements of aboveground plant size into estimates of dry biomass using species- or functional group-specific allometries created for each site and season (Huenneke et al. 2001, Rudgers et al. 2019). See Rudgers et al. (2019) for full description of how current allometric models were constructed. Because this system primarily receives precipitation in the form of winter and monsoon precipitation, bimodal patterns of annual plant growth occur. We made observations in both the spring (April/May) and fall (September/October) to capture peak biomass production in both seasons. At the desert grassland site, we did not record plant abundance data in 2010, 2017, or the spring of 2018. In these seasons, species' biomass was estimated using linear relationships between the abundance of that species at nearby sites with similar fire-disturbance histories.

We calculated seasonal metrics of community structure or species' abundance by first averaging the aboveground biomass of each species across the replicated fixed-position plots at the site. Because we compared both community structure and individual species abundance to flux measurements that aggregated the entire ecosystem into a single measure of carbon entering or leaving the ecosystem, we felt that it was appropriate to summarize the sixteen to twenty m^2 plots at each site. When calculating community structure metrics, we only included species that contributed at least 0.05% g/m^2 of aboveground biomass to reduce the influence of very rare and improbable-to-sample species. We calculated seasonal species diversity with the *community_diversity()* function from the R package *codyn* (Hallett et al. 2016), using the metric "Shannon" which calculates the Shannon diversity index. We calculated seasonal species richness and evenness with the *community_structure()* function in *codyn*, using the metric

"SimpsonEvenness". The abundance of the dominant species was calculated simply as the average biomass (g/m^2) of either black grama grass or creosote bush in the desert grassland and creosote shrubland, respectively. We used biomass as a proxy for abundance because individual plants are not consistently differentiated in the Sevilleta LTER long-term data and individual plants are difficult to differentiate in these species. We calculated the abundance of the entire community as the sum of average aboveground biomass (g/m^2) for each species at each site.

2.2.3 Carbon flux and micrometeorological measurements

We measured net ecosystem exchange of CO_2 (NEE) at each site using tower-based eddy covariance. At each site, a 3-D sonic anemometer (Model CSAT3, Campbell Scientific Inc., Logan, UT, USA) and open path infrared gas analyzer (IRGA; Model LI-7500, LI-COR Inc., Lincoln, NE, USA) mounted at 3m above ground level, measured the three-dimensional vectors of wind velocity, sonic temperature, water vapor, and CO_2 density, sampled at 10Hz by a datalogger (CR3000, Campbell Scientific). Post-processing of the tower high-frequency data included filtering, despiking, and coordinate rotation (Anderson-Teixeira et al. 2011b). We calculated half hourly fluxes, and applied both the Webb-Pearman-Leuning correction for open-path instruments (Webb et al. 1980), and frequency correction (Massman 2000). We stored data both wirelessly and as a hard copy on an SD card. All data streams were regularly monitored for quality and instrumentation was calibrated as needed. We partitioned net carbon fluxes into gross primary productivity (GPP) and ecosystem respiration (R_e) components using Lasslop et al. (2012). We used fluxes measured from January 2010 - December 2019 at both sites for this study.

We also measured meteorological factors such as radiation, PAR, air temperature, humidity and precipitation. Incoming radiation (both long- and short-wave) was measured with a CNR1 4-way Kipp & Zonen net radiometer (Kipp & Zonen). We measured relative humidity and air temperature with an HMP45C Vaisala temperature/relative humidity probe (Vaisala Instruments, Helsinki, Finland) and used these values to calculate vapor pressure deficit. Incoming photosynthetically active radiation was measured with a Kipp & Zonen LI-190 PAR sensor (LICOR, Lincoln, NE, USA). These sensor data were continuously measured at 10Hz frequency and stored as 30-minute averages. Precipitation, recorded as a 30-minute sum, was measured using a TE525 Texas Electronics 6" tipping bucket rain gage (Texas Electronics, Dallas, TX, USA).

We smoothed the carbon flux time series and vegetation indices using a 9-day rolling median window. We calculated seasonal GPP and R_e as the sum of each respective flux in the 90 days prior to biomass sampling for each season. This incorporated the spring and monsoon growing season each year. Precipitation was summed across 45-day-wide rolling windows throughout the entire ten-year time series. We determined that 45 days was a biologically meaningful window size because it maximized the correlation between daily carbon fluxes and vegetation indices.

2.2.4 Repeat digital photography

We used two Moultrie I-40 game cameras (Pradco Outdoor Brands, Birmingham, AL, USA) to take photos in both sites between April 2010 and August 2013. In 2010, these cameras took one photo per day at noon. In subsequent years, photo acquisition increased to one image/hour during all daylight hours. Cameras were located 10-60 m from the flux

tower, facing west. In November 2014, we started using StarDot (NetCam SC IR, StarDot Technologies, Buena Park, CA, USA) cameras placed within 50 m of each flux tower, facing north. These cameras took visible-spectrum and near-infrared channel photos every 30 minutes. These photos are archived and available on the PhenoCam Network website (under US-Seg and US-Ses).

Figure 2.1. Images from the desert grassland (left) and creosote shrubland (right) sites. In the desert grassland, almost all of the grasses are black grama grass and the dark green subshrubs are snakeweed. In the creosote shrubland the dark green shrubs are creosote bush and the patch of grass in the center of the image is intermixed black grama, James' galeta, and sand dropseed grasses.

Here, we use photos taken between the hours of 08:00 and 16:00. All cameras experienced some degree of drift and slight scene shifts. To account for this, we co-registered all photos into aligned series using a combination of manual and automated processing techniques. We used Matlab (version R2019a, The Mathworks Inc., 2019) for all photo pre-processing, including automated image co-registration and analysis of image coloration was done in Matlab. We used R (version 4.0.3, R Development Core Team, 2020-10-10) for data summarization and analysis.

We used a standard vegetation index (Green Chromatic Coordinate; GCC) to quantify plant phenology from camera images. At our arid study sites, the high proportion of visible bare ground within each scene makes manually selecting vegetated regions of

interest (ROI's) challenging. In addition, the characteristic rapid growth, wilting, and senescence that occurs throughout the year in drylands make choosing static ROI's that exclude gray or tan leaf litter difficult. Therefore, we used an automated method to retrieve only the green pixels, representing photosynthetically active material, from each photograph. For all regions of interest, we calculated the GCC value of each pixel and removed pixels with GCC values less than 0.33. This allowed us to eliminate pixels representing bare ground, dead plant material, blue sky, and man-made objects such as poles and flagging. We then calculated the average GCC value of the remaining pixels within each ROI. We smoothed the vegetation index and carbon flux time series using a 9-day rolling median window. GCC time series for each ROI type, like carbon fluxes, were smoothed using a 9-day rolling median window. Because the GCC values from the two camera models had different magnitudes, we scaled the GCC values from each ROI-type from each camera between 0 and 100.

Due to periodic camera failure, there were sometimes gaps in GCC time series that corresponded to the dates when biomass was measured at the sites (dates indicated by vertical bars in Fig. 1.1). Because of this, we correlated seasonal community metrics with the peak GCC value occurring within 30 days of biomass measurements.

Figure 2.2. An example of how color thresholding isolated green pixels from an image of the desert grassland site. The original image is shown on the left and a GCC-thresholded image is shown on the right.

2.2.5 Analyses

We used simple linear models to compare seasonally summed carbon fluxes to metrics of community structure or biomass. To compare daily time series of fluxes to vegetation indices, we used general least squares model that included an autoregressive (AR1) term from the package *nlme* in R. Model fits were compared using the Akaike information criterion (AIC). For each set of model comparisons, the same number of predictor values were used, with no missing data permitted. We evaluated the difference in AIC values for each set of models and the model with the lowest AIC value (delta AIC of 0) was determined to be the winning model. Models with delta AIC values less than two were not appreciably different from the winning model and were treated as tied for winning model.

2.3 Results

2.3.1 Time series of GCC, carbon fluxes and biomass

Across the ten-year study period, vegetation indices, ecosystem carbon fluxes, and direct biomass measurements captured plant productivity across a range of climatic conditions (Fig. 2.3). Precipitation fell in stochastic pulses, with most rainfall occurring in the fall monsoon season (Fig. 2.3A). Vegetation indices (Fig. 2.3B) showed stochastic plant growth patterns, with some pulses of growth lasting only a few weeks. In the creosote shrubland, vegetation indices also illustrate the steep decline in community greenness following a severe freeze event (Feb. 2011) and subsequent drought (2011-mid 2013). Ecosystem carbon fluxes in both sites were largely limited to April-October, with distinct pulses visible in the spring and summer of each year (Fig. 1C). Direct measurements of aboveground biomass (Fig. 2.3D) suggest season to season variability was large, with some seasons having nearly ten-fold more biomass than others. Aboveground biomass was especially low after the freeze disturbance (Feb. 2011) in the creosote shrubland and wildfire (Aug. 2009) in the desert grassland sites until the very wet monsoon season of 2013.

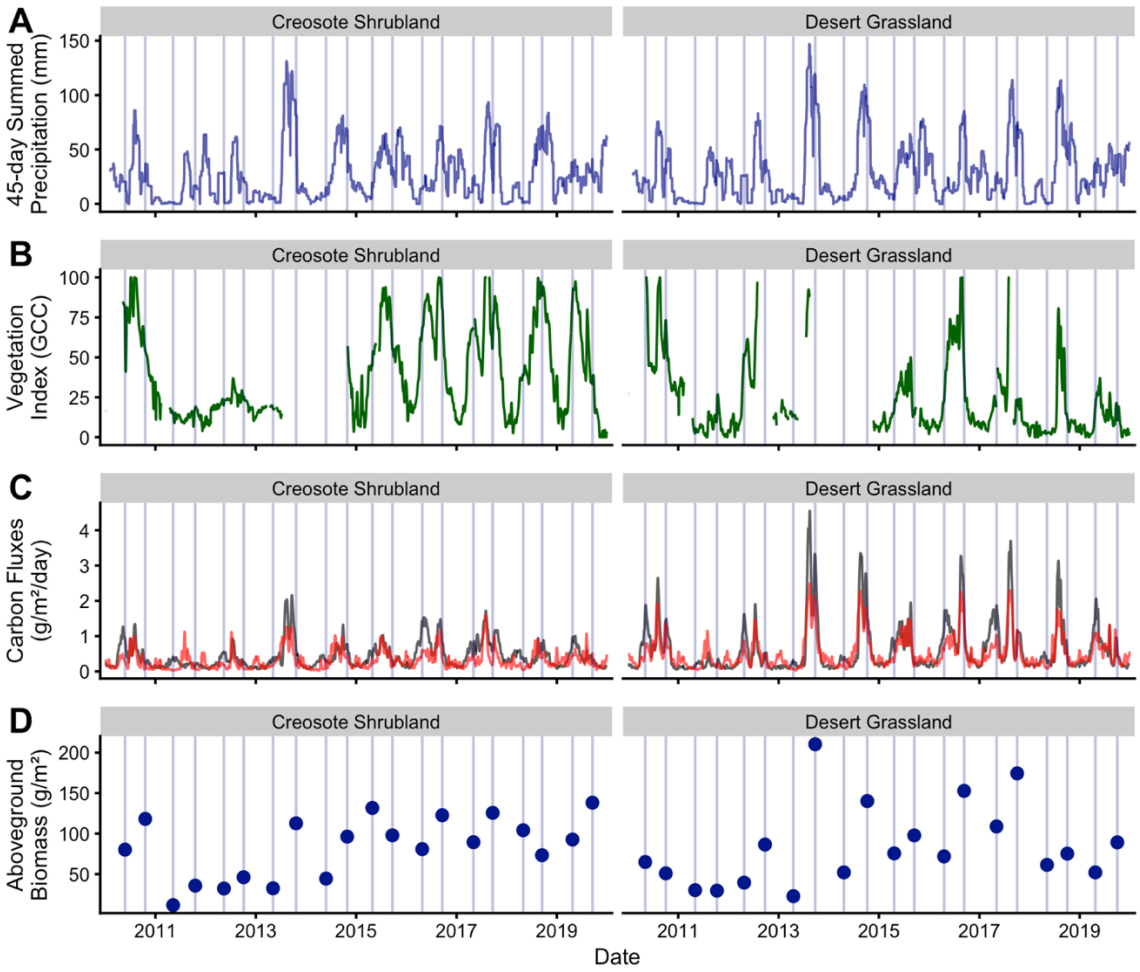

Figure 2.3. Time series of precipitation (45-day rolling sum; mm), vegetation indices (GCC), carbon fluxes (black line is GPP and red line is RE in g C/m^2/day), and measured biomass (three ways to measure productivity). Blue vertical lines represent timing of direct biomass measurements.

2.3.2 Ecosystem carbon fluxes driven by dominant species

In the desert grassland, ecosystem carbon fluxes, both GPP and RE, were significantly correlated with species richness and species evenness, but not species diversity (Table 2.2; Fig. 2.4). Although there were more species present when fluxes of carbon fixation and respiration were large, the relationship between carbon fluxes and species evenness was negative, indicating that the largest carbon fluxes occurred when the system was more dominated by one or a few species. Model comparison tests

between the three metrics of community structure determined that the negative relationship with species evenness was the best predictor of both GPP and RE (comparing predictor metrics richness, diversity, and evenness in Table 2.2). At the grassland site, carbon fluxes were significantly and positively correlated with both the aboveground biomass of the dominant plant species and the entire plant community. When abundance metrics were included in model comparisons, the biomass of black grama grass alone was a better predictor of both GPP and RE than community structure metrics or the biomass of the entire plant community (comparing all five predictor metrics in Table 2.2).

In the creosote shrubland, community structure predicted less variability in seasonal carbon fluxes than in the desert grassland site (Table 2.2; Figure 2.4). Like the desert grassland, shrubland carbon fluxes were positively correlated with species richness, negatively correlated with evenness, and not correlated with species diversity (comparing predictor metrics richness, diversity, and evenness in Table 2.2). Model comparisons between community structure metrics determined that species richness and evenness were tied for best predictors of both GPP and RE. The seasonal aboveground biomass of creosote bush and the entire community were both significantly and positively related to carbon fluxes. When abundance metrics were included in model comparisons, the summed biomass of the whole community was the best predictor of both GPP and RE (comparing all five predictor metrics in Table 2.2).

Table 2.2. Linear model summaries of carbon fluxes (GPP or RE) predicted by community structure indices (species richness, Shannon diversity index, or Simpson's evenness) and average aboveground biomass (g/m^2) of the entire community or the dominant species in each site. Asterisks in the p-value column indicate the model slope was significantly greater than 0 at the 0.95 α-level. Bold rows indicate the model with the best fit, as determined by AIC.

Site	Carbon flux	Predictor metric	Model intercept	Model slope	Model fit (R^2)	P-value	AIC
desert grassland	GPP	richness	5.1	6.9	0.341	0.009*	200.3
		diversity	102.6	-22.3	0.021	0.557	207.8
		evenness	**159.9**	**-383.8**	**0.496**	**0.001***	**195.2**
		community biomass	18.2	0.7	0.570	<0.0001*	192.1
		black grama biomass	**11.6**	**1.2**	**0.682**	**<0.0001***	**186.4**
	RE	richness	15.0	4.9	0.286	0.018*	191.8
		diversity	94.5	-26.4	0.049	0.365	197.3
		evenness	**130.1**	**-299.3**	**0.510**	**0.001***	**184.7**
		community biomass	22.8	0.5	0.512	0.001*	184.6
		black grama biomass	**15.1**	**0.9**	**0.686**	**<0.0001***	**176.2**
creosote shrubland	GPP	**richness**	**5.4**	**2.9**	**0.231**	**0.032***	**193.5**
		diversity	45.7	7.7	0.008	0.703	198.5
		evenness	**69.5**	**-113.1**	**0.182**	**0.061**	**194.7**
		community biomass	**8.4**	**0.5**	**0.454**	**0.001***	**186.6**
		creosote biomass	19.3	0.5	0.324	0.009*	190.9
	RE	**richness**	**12.1**	**1.8**	**0.173**	**0.068**	**180.2**
		diversity	40.0	0.947	0.000	0.946	184
		evenness	**51.5**	**-75.4**	**0.168**	**0.073**	**180.3**
		community biomass	**13.6**	**0.3**	**0.346**	**0.006***	**175.5**
		creosote biomass	19.8	0.3	0.257	0.022*	178.1

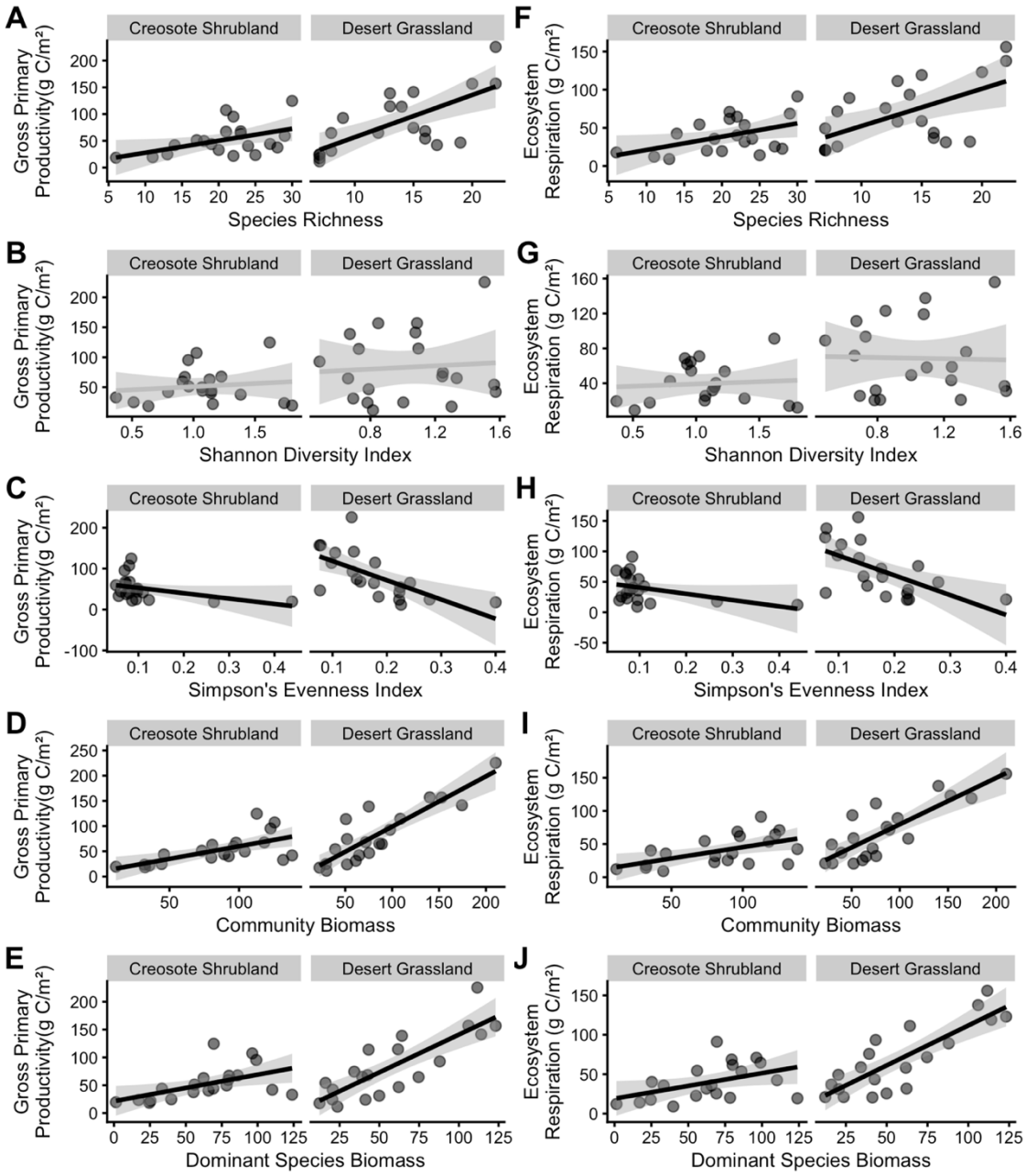

Figure 2.4. Seasonal community structure (A and F: species richness, B and G: Shannon diversity index, C and H: Simpson's evenness index) or summed biomass (D and I: community biomass, E and J: dominant species biomass) versus seasonally-summed gross primary productivity (A-E) or seasonally-summed ecosystem respiration (F-J). Black lines represent linear fits with shaded 95% confidence estimates. Grey lines represent non-significant linear fits.

2.3.3 Phenology of common species and carbon fluxes

Vegetation indices and ecosystem carbon fluxes varied similarly throughout the year (Fig. 2.5). The phenological activity of dominant species explained more of the

variability in ecosystem carbon fluxes than that of subordinate species, but only in some months (Fig. 2.6). In the desert grassland site, black grama grass VI explained more of the variability in ecosystem-level GPP and RE in peak monsoon growth months (July-September). In spring and late fall (March-June and October-November), snakeweed phenology or the average phenology of the entire community were most correlated with ecosystem GPP and RE.

In the creosote shrubland site, the phenology of creosote bush explained more of the variability in ecosystem-level GPP for most of the year, and especially in the spring season. During the latter part of the monsoon season (August-November the average phenology of the entire community was a better predictor of GPP. Patterns were similar when comparing phenology to RE.

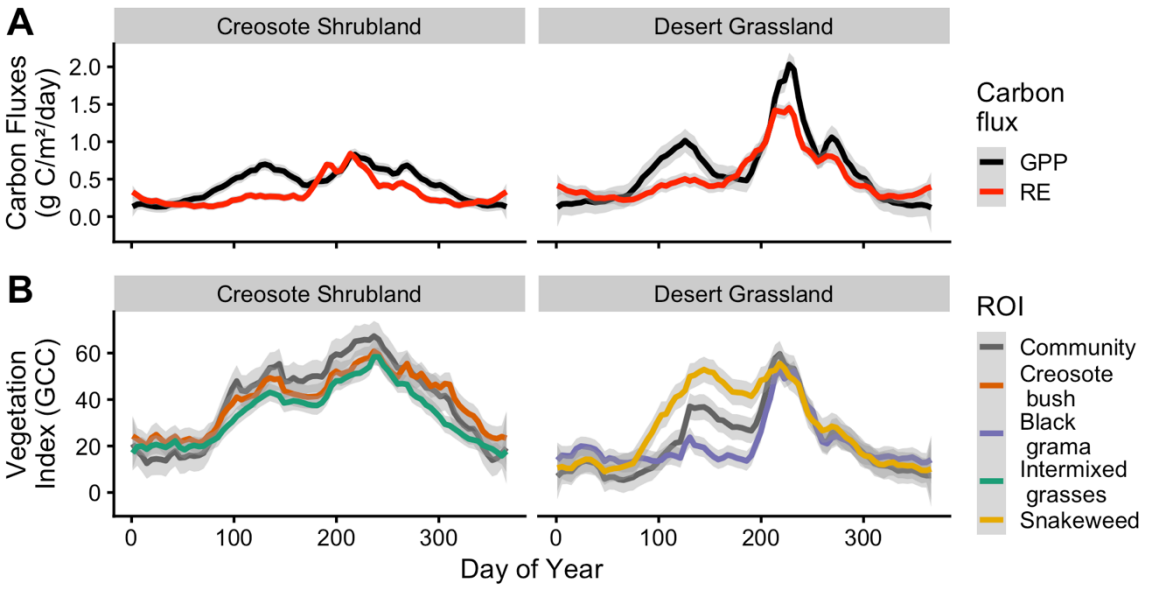

Figure 2.5. Time series of average daily carbon fluxes throughout the year (A) and average daily vegetation index (GCC) of plant groups (ROI's) throughout the year (B).

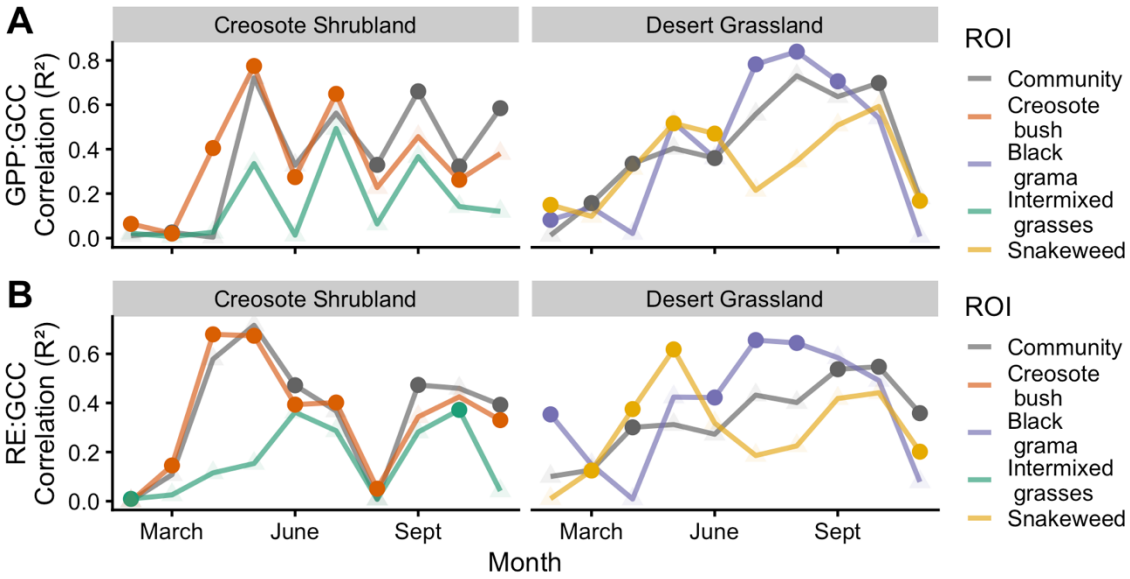

Figure 2.6. Time series of monthly pseudo-R^2 values from generalized least squared models predicting daily carbon fluxes (A: gross primary productivity, B: ecosystem respiration) using daily vegetation indices (scaled GCC), after taking temporal autocorrelation (AR1) of daily carbon fluxes into account. Filled circles indicate the plant group (camera ROI) phenology that best modelled the carbon flux in that month.

2.3.4 Temporal divergence in climatic influences

Species varied in sensitivity to climate throughout the year (Fig. 2.7). In the desert grassland site, black grama greenness increased with precipitation in the monsoon rainy season, July-September but decreased with hot temperatures in July and August. In comparison, the phenology of snakeweed was most related to rainfall patterns in spring.

In the creosote shrubland site, the phenology of creosote bush and dominant grasses (intermixed black grama, James' galeta, and sand dropseed grasses) showed similar sensitivities to climate. The only exception is that creosote bush phenology responded slightly more positively to precipitation in spring (April and May) and late fall (October-November).

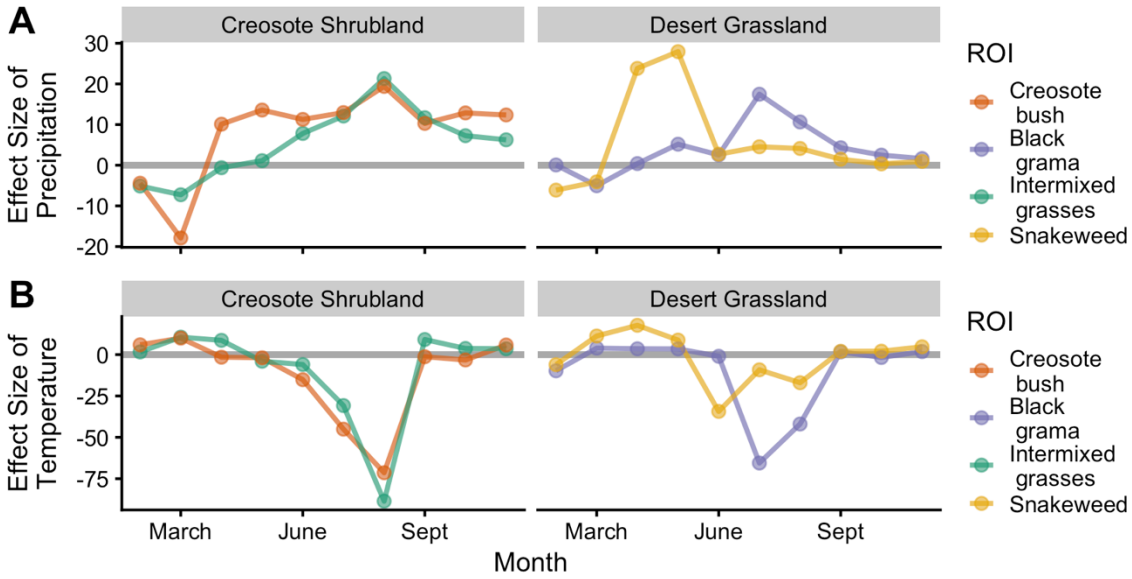

Figure 2.7. Effect size of 45-day accumulated precipitation (A) and air temperature (B) on vegetation indices (daily GCC). Effect size here is the slope of linear regressions between GCC (scaled between 0 and 100 for each species) and z-scored climate variables.

2.4 Discussion

We were able to capitalize on the coupling of eddy covariance flux sensors, micrometeorological measurements, cameras, and direct observations of plant community composition to link ecosystem structure and function in these drylands. Using this framework, we found that the abundance of the dominant species was a much stronger predictor of ecosystem carbon fluxes than community diversity in our Chihuahuan Desert grassland and shrubland study sites, providing strong support for the mass-ratio hypothesis in these dryland biomes. Interestingly, the daily-scale phenology of the dominant species only explained the majority of daily carbon uptake and respiration in some seasons.

In dryland biomes in general, species differ in phenology (Huang et al. 2019) and grow in multiple pulses throughout each year (Noy-Meir 1973), creating variable community structures and dynamic ecosystem functioning. Our study period encompassed ten years of natural variability, including natural disturbance events – fire, freeze, and

drought – that caused greater than ten-fold reductions in the biomass of dominant species. This variability in community structure allowed exploration of the relationship between abundance and diversity of plant species to the functioning in these ecosystems.

2.4.1 Dominant species influence ecosystem carbon fluxes

The importance of dominant species driving ecosystem productivity in these biomes is similar to previous studies which found that dominant species preserved community productivity after subordinate and rare species were removed (Smith and Knapp 2003). In addition, the increase in community productivity with both the abundance of the dominant species and species richness, but not diversity, is similar to Baer et al. (2004). Our findings further suggest that dominant species can play foundational or faciliatory roles in natural systems, remaining principal even as species richness increases. Previous work in this region showed that aboveground productivity did not recover for over a decade after the removal of black grama grass and creosote bush (Peters and Yao 2012). This suggests when dominant species are disturbed or extirpated in these biomes, no other species can compensate, at least in terms of productivity. These dominant species may be better able to access nutrients efficiently, withstand harsher conditions, or support more positive plant-soil interactions than subordinate species in the system (Lavorel and Garnier 2002, Orwin et al. 2010, Chung and Rudgers 2016, Saiz et al. 2019).

While previous studies have found a positive relationship between evenness and productivity, these were in more mesic grasslands where the dominant species was experimentally controlled (Mulder et al. 2004, Orwin et al. 2014). In both of our dryland sites, evenness was a strong, negative predictor of ecosystem carbon fluxes in both the

grassland and shrubland sites. Notably, our dryland sites retained a single dominant species across our study period whereas more mesic grasslands often have several co-dominant species or congeners that become dominant in the face of disturbance (Silletti and Knapp 2002). Unlike Mulder et al. (2004), we also found that species richness increased with abundance of the dominant species, both increasing in wetter years. This suggests that resource limitation is a much stronger constraint on growth and abundance than competitive exclusion (Chesson et al. 2004). Our comparative assessment of community structure metrics allowed us to differentiate between the importance of the number, identity, and abundance of species on ecosystem functioning (Smith and Wilson 1996).

2.4.2 Temporal complementarity of phenology and climactic associations

Temporal differences in vegetative phenology and resource use among species can explain how ecosystem services are maintained throughout each year. Although the dominant species at our sites were perennial and consistently the most abundant species in the peak of the spring and monsoon growing seasons, the phenology of these species did not explain the variation in daily carbon fluxes in every month. In the desert grassland, the phenology and biomass of the dominant C_4 grass explained more of the variability of carbon fluxes in the peak of the hot, rainy growing season. In the creosote shrubland, the dominant C_3 shrub was a better predictor of fluxes in the spring growing season. Subordinate species in both of these systems may be able to avoid direct competition with dominants by growing in the portions of the year not favored by the dominant species, and thus contribute more to ecosystem carbon fluxes during those times (Chesson 2000).

The sensitivity of vegetative phenology to climate was generally highest in months when the carbon flux: vegetation index relationship was strongest for each species. At both sites, the growth of C_4 grasses generally responded strongly to monsoon precipitation, but this response was weaker when conditions were very hot. At both sites, C_3 shrubs grew more in warm, wet springs. Some studies have found weaker correlations between community productivity and annual climate within sites than between sites on large scales (Sala et al. 2012, Wilcox et al. 2016). We found that the productivity of influential species was sensitive to climate on sub-annual time scales and the timing of sensitivity varied between functional groups. Therefore, interannual turnover of species would result in a different cohort of species, with different seasonal climate sensitivities, resulting in a weaker relationship between annual climate variables and community-wide productivity. Exploring the abiotic constraints of growth of the most common species may lead to a better understanding of aggregated ecosystem productivity and how it may change in light of future climate changes, even on sub-annual time scales.

As climate continues to warm in the arid Southwest U.S., we expect to see less primary productivity in the warm monsoon growing season. At both of our study sites, the vegetative phenology of common species responded negatively to warmer temperatures. The negative effect of temperature was stronger than the positive effect of precipitation for all species. Especially in desert grasslands, the depressed growth of C_4 grasses in the monsoon season could detriment ecosystem-wide carbon fluxes.

A constraint of our approach was that we only tracked relatively large, perennial and consistently abundant species rather than smaller, more ephemeral species in camera

images. Camera placement and ROI selection can enhance the ability of PhenoCams to understand species or ecosystem productivity by increasing visibility of specific species.

2.4.3 Conclusions

Our findings demonstrate the importance of teasing out the relative effects of community diversity, evenness, and species identity on ecosystem-scale functioning (Gitlin et al. 2006, Felton and Smith 2017). Especially in the face of anthropogenic habitat destruction and climate change, which are causing unparalleled extinctions, there is an urgent need to continue examining the impact of changing species abundance on ecosystem functioning (Cardinale et al. 2012). In our semi-arid study sites, the abundance of the dominant plant species was important in predicting not just community productivity, but the total carbon uptake and respiration of the entire ecosystem.

Chapter 3

Plant phenology predicts population stability in semi-arid biomes

Authors: Alesia J. Hallmark[1], Scott L. Collins[1], Marcy E. Litvak[1], Jennifer A. Rudgers[1]

[1] Department of Biology, University of New Mexico, Albuquerque, NM, USA

3.1 Introduction

The temporal stability of population abundance can affect the presence and magnitude of biotic interactions (Visser and Holleman 2001, Elzinga et al. 2016), access to resources, and potential exposure to biotic and abiotic stressors (Harrison 1979, Griffith and Watson 2005). Population stability is related to life history strategies and fundamentally differs among species and between communities (Chesson et al. 2004, Angert et al. 2007). Population instability has been linked to population declines due to environmental perturbations and large environmental stochasticity (Ma et al. 2020). Less stable populations are more likely to become asynchronized with populations that maintain stable abundances over time, potentially creating mismatches between partners in mutualistic or predatory interactions (Zhang et al. 2016). Alternatively, the opportunistic growth that contributes to instability can be an adaptive strategy to maximize fitness (Pilson 2000, Chesson et al. 2004). Furthermore, temporal asynchronies in species abundances can promote coexistence among competitor species (Chesson 2000) and also drive stability in ecosystem function (Ovaskainen et al. 2013). Therefore, the ability to predict population stability could provide inferences for a range of biotic interactions, underlying mechanisms

of species coexistence, and predicted sensitivity to future perturbations, such as climate change.

Species traits may predict population stability. Therefore, deciphering the links from traits to stability could facilitate the development of a mechanistic framework to predict temporal stability in population abundance. For example, plant species with greater leaf dry matter content, a conservative growth strategy, had more stable population sizes over time, which reduced variability in productivity of the plant community as a whole (Polley et al. 2013, Májeková et al. 2014). Few experimental studies (e.g., MacGillivray and Grime 1995, Sauer and Link 2002, Polley et al. 2013) have connected specific traits with population stability (Adler et al. 2006, Angert et al. 2009), perhaps because of the difficulty of obtaining long-term data on stability for many species. Practically, traits could be effective stand-ins in the absence of long-term data on population stability, which are labor-intensive to collect. Traits are easier to catalogue than long-term population dynamics, especially for rare, unstable species that appear infrequently.

Phenology is one aspect of trait ecology that has not been linked to temporal stability but may be a key determinant. Broadly, phenology is defined as the timing of important life events such as birth or germination, maturation, and reproduction (Forrest and Miller-Rushing 2010). Phenology influences demography by creating matches or mismatches in timing with critical abiotic events or with interacting species (e.g., pollinators, seed dispersers) (Miller-Rushing et al. 2010). Although many studies have linked shifts in phenology to temporal trends in productivity or abundance over time (Richardson et al. 2010, Duveneck and Thompson 2017), these studies did not use phenological traits to explain the temporal stability of population size.

We propose that phenology could govern population stability in two, alternative scenarios. First, species with longer phenophases (i.e., observable phenological periods that have discrete beginning and endpoints), such as a long period of active growth or fruiting in plants, may have traits that enable them to withstand a broad range of environmental conditions (Moussus et al. 2011), thereby stabilizing population size. For example, a long window of fruiting could offset costs associated with mismatches in the timing of active animal seed dispersers. Similarly, bird populations with longer reproductive periods (more clutches per year) were less sensitive to changes in the timing of peak food availability (Jiguet et al. 2007). Species with shorter phenophases may have less time to accumulate resources and reproduce successfully. Second, longer phenophases may destabilize populations because species are exposed to a wide range of abiotic and biotic conditions, exposing them to the risk of extreme events that cause temporal instability in abundance. For example, experimental warming increased the length of the growth phenophase for several tree species but also caused trees to suffer more damage from a late freeze event than trees growing in un-warmed controls (Richardson et al. 2018).

Phenology is often tightly coupled to climate variables (Forrest and Miller-Rushing 2010, Primack and Miller-Rushing 2011), creating a mechanistic link between climate and population stability. For example, climate warming is not only altering the timing of phenology globally but also affecting local species abundance and temporal synchronies among interacting species (Parmesan and Yohe 2003, Ovaskainen et al. 2013, Thackeray et al. 2016). Understanding climate drivers of phenology may therefore improve predictions on future instabilities in population abundance under climate change. For example, climate warming may result in longer growing seasons for species in which

vegetative phenology is constrained by low temperatures, but generate more variable growing seasons in species that require winter chilling before spring leaf-out (Morin et al. 2009). Climate likely influences specific phenophases more than others, depending on the sensitivity of each phenophase to temperature or precipitation. We predict that when a phenophase closely tracks climate, particularly in systems where climate is highly stochastic, climate-driven variability in phenology is likely to play a key role in population temporal stability. This is an important hypothesis to evaluate because temporal variability is often missing from ecological forecasts (Cárdenas et al. *in review*, Harris et al. 2018), such as ecological niche models that capitalize on space-for-time substitution to predict future changes in species abundance and distributions (Melo-Merino et al. 2020). Temporal variability in phenological traits that characterize climate niches is rarely incorporated into such forecasts, despite known inaccuracies in the space-for-time substitution approach (Harris et al. 2018, Kazenel et al. 2019).

Different phenophases may rank more importantly in predicting population stability because species face trade-offs in allocation among life history stages, such as vegetative growth versus reproduction (Stearns 1992). For example, past work has compared relative plant investment in leaf economics (e.g., leaf dry matter content) and found that species with more conservative vegetative strategies had higher water use efficiency and more stable populations over time (Angert et al. 2009, Májeková et al. 2014). However, reproductive traits may also be important predictors of stability in species for which population growth is governed primarily by reproduction and recruitment, rather than growth or survival. For example, in masting plants, which fruit episodically, population explosions should follow mast years, generating large temporal instability in

population size over time (Kelly and Sork 2002). Differential investment in the duration of the active vegetative growth period versus the reproductive period could be an important phenological mediator of population stability.

The stochastic climates of drylands provide useful testbeds for evaluating the influence of phenological traits on population stability. Drylands cover 45% of Earth's land surface (Prăvălie 2016), support nearly 40% of the human population, and are expanding in extent as climate warms and dries (Burrell et al. 2020). A key ecological challenge in drylands is stochastic water availability, which can drive large variability in phenology (Beatley 1974, Peñuelas et al. 2004, Crimmins et al. 2011). For example, desert plants may attempt to flower multiple times in a season, but abort most flowers before successfully fruiting (Crimmins et al. 2013). Similarly, for some species, the onset and duration of the vegetative phenophases may be mediated by the ability to acquire and store water (i.e. rooting depth, water storage capacity) or antecedent growth (Beatley 1974, Crimmins et al. 2011, Ogle et al. 2015). Although some species are adapted to these unpredictable conditions, dryland climates are becoming increasingly more arid and variable over time (Rudgers et al. 2018, Maurer et al. 2020). For example, in the southwestern U.S., interannual variability in the drought index has increased, rainfall events have become smaller and more frequent, and the onset of the rainy season is occurring later in the year (Gutzler and Robbins 2010, Petrie et al. 2014, Rudgers et al. 2018). Thus, the high stochasticity of dryland ecosystems enables us to leverage natural variability over time (Ridolfi et al. 2011, Ibáñez et al. 2013) to detect patterns indicative of key roles for phenological traits in stabilizing population dynamics.

Here, we asked the question: Do species' phenological traits predict temporal stability in population abundance? To address this question, we paired 18 years of monthly phenology observations with biannual biomass measurements for 98 species from semi-arid grasslands and shrublands, monitored by the Sevilleta Long-Term Ecological Research program in central New Mexico.

3.2 Methods

3.2.1 Site Description

This study took place in the Sevilleta National Wildlife Refuge (SNWR) in central New Mexico, USA. SNWR lies at the confluence of several biomes, including three studied here: Chihuahuan Desert grassland (34.3331, -106.736), Chihuahuan Desert shrubland (34.3331, -106.736, and Great Plains grassland (34.3348, -106.631). The elevation at these sites ranges from 1615-1670 m. Mean annual precipitation during our study period (2002-2019) was 240.4 ± 7.8 mm, with most precipitation falling during the monsoon season (July-October). Mean annual temperature was 14.5°C and mean standing plant biomass was 88.9 ± 7.2 g/m^2. Plant phenology, plant abundance, and meteorology data were collected similarly at all sites.

3.2.2 Plant phenology data

Plant phenology was recorded monthly by trained observers along four 200 m length × 2 m width belt transects at each site. Within each belt, every plant species present was noted. For up to ten representative individuals of each species, vegetative phenology was scored as "N" (new green leaves growing), "O" (only older, but still green, leaves

present), “B” (leaves browning), or “Z” (no leaves present). Reproductive phenology was scored as “B” (flower buds present), “Fl” (open flowers present), “Fr” (ripe fruit present), or “Z” (no reproductive structures present). Observations were made within a few days of the first calendar date of each month. Phenology time series included the same number of years for each replicate belt transect, beginning January 2002 and ending December 2019.

Phenological traits were first calculated for every species within each replicate web. Onset dates were determined as the first Julian day when at least one-quarter of the individuals of a species on the belt transect entered a phenophase (i.e., produced new leaves, flowers, or fruits). Similarly, offset dates were calculated as the last Julian day when at least one-quarter of the individuals of a species on the belt transect remained in a phenophase. The duration of each phenophase was then calculated as the number of days between the onset and offset of the phenophase. Over half of the species evaluated produced fruit within 60 days of leaf-out. We therefore determined that a population could have reached maturity but failed to fruit on a transect when it was observed with new leaf growth in at least two monthly observations within a year, but there were zero observations of fruiting. Phenological traits of each species were then averaged across replicate transects (maximum of 12 transects per species per year). Averaging phenological traits for each species across the full time series and over the three distinct, adjacent ecosystem types best accounted for phenological plasticity within each species (see also Májeková et al. 2014) and possible genetic structuring within subpopulations (Hendry and Day 2005).

3.2.3 Population stability data

Plant growth in many dryland ecosystems is annually bimodal, tracking winter precipitation and monsoon rain pulses. Thus, to capture peak seasonal plant production, we made biannual observations of plant species biomass in spring (April/May) or fall (September/October). These plant abundance data were recorded within 1 m^2 fixed-position quadrats at each site using non-destructive methods (N = 248 quadrats). Within these quadrats, every plant was identified to species. Ground cover (m^2) and maximum height of live tissue (cm) was recorded for each individual plant per quadrat. These size measurements were then converted into estimates of dry aboveground biomass using species- or functional group-specific allometries created for each site and season (Muldavin et al. 2008, Rudgers et al. 2019). Rudgers et al. (2019) provides a full description and R scripts for the allometric model construction used in our analyses.

We calculated population stability for each species as the coefficient of variation (CV = standard deviation divided by mean) of all biannual estimates of plant biomass. CV is an effective and commonly used metric of population stability for cross-species comparisons because units of population size (e.g., differences in biomass among species) are removed from the estimate of stability (Kindvall 1996). The CV of biannual biomass and maximum annual biomass were highly correlated ($F_{1,92}$ = 1893.0, R^2 = 0.95, $P <$ 0.0001, see Supplemental Appendix B, Fig. B1). We reported results for seasonal patterns.

3.3.4 Meteorological data

Precipitation and temperature were measured at independent meteorological stations at each site. Any missing data (resulting from temporary equipment failure) were

gap-filled with modelled data constructed by comparing long-term (18-32 year) records from nearby met stations within the SNWR (see also Rudgers et al. 2018). Data were aggregated into monthly averages (average mean daily air temperature) or sums (total monthly precipitation), then paired with phenological observations made at the end of that calendar month (e.g., total precipitation that fell in April was paired with phenology observations made on May 1st of that year).

3.3.5 Phylogenetic relationships

For each plant species, we recorded functional group (grass, forb, shrub, tree), life-history strategy (annual, annual/biennial, perennial), and photosynthetic pathway (C_3, C_4, CAM) from the USDA Plants Database (USDA, NRCS 2020). We used observations from 63 C_3 species, 30 C_4 species, and 6 CAM species. Our dataset included 29 annual or annual/biennial species and 69 perennial species, and 64 forb, 21 grass, and 13 shrub or tree species.

Phylogenetic signal: To assess the degree to which closely related plant species shared similar relationships between phenological traits and population stability, we pruned the time-calibrated 31,383-species Qian and Jin (2016) plant phylogeny to include focal plant taxa (details in Supporting Information). For the magnitude of phylogenetic signal in phenology as a predictor of stability, we calculated phylogenetic signal as Pagel's λ (Pagel 1999) using the R function *phylosig*() in the package *phytools* (Revell 2012). We evaluated relationships between phenological traits and population stability by accounting for evolutionary history using phylogenetically independent contrasts (*PIC*s) (Garland et al. 1992). We obtained *PIC*s using R package <ape> (Paradis and Schliep 2019) with the

general linear models described next. Analyses used original branch lengths in millions of years, but alternative analyses assuming all = 1 or Grafen branch lengths produced qualitatively similar results (results not shown).

3.3.6 Statistical analyses

To compare the relative importance of alternative phenological traits as predictors of population stability, we used general linear models for each species. Models took the form of: *CV* of biannual aboveground biomass ~ phenological trait, with plant species (or the *PIC*) as the unit of replication. Model selection procedures ranked the relative importance of phenological traits using the relative fit of each model to the data from maximum likelihood estimation and the second order Akaike Information Criterion (*AICc*) (Burnham and Anderson 2002). We used model selection procedures rather than multiple regression analyses because some phenological traits were highly correlated (Supplemental Appendix B, Fig. B2), and because our aim was to rank the relative importance of phenological traits rather than dissect possible interactions among covarying traits. All analyses were conducted in the R programming language (R Core Team 2020).

3.3 Results

3.3.1 Phenological traits predict plant population stability

Species with more temporally stable populations had longer vegetative phenophases (Fig. 3.1A), meaning they maintained green leaves for more days of the year ($F_{1,96}$ = 51.85, R^2 = 0.35, $P < 0.0001$). Temporally stable plant species also had longer reproductive phenophases than more variable populations (Fig. 3.1B, $F_{1,95}$ = 9.5, R^2 = 0.09,

$P = 0.003$). One foundation plant species had an exceptionally long fruiting period (*Larrea tridentata*, creosote bush). However, exclusion of that dominant species from the analysis still resulted in a significant correlation ($F_{1,94} = 4.74$, $R^2 = 0.05$, $P = 0.032$). More stable populations also started producing new leaves earlier in the year than less stable populations (Fig. 3.1C, $F_{1,96} = 16.44$, $R^2 = 0.15$, $P = 0.0001$). Finally, more stable populations waited longer to begin the fruiting phenophase (Fig. 3.1D, $F_{1,96} = 15.66$, $R^2 = 0.14$, $P = 0.001$).

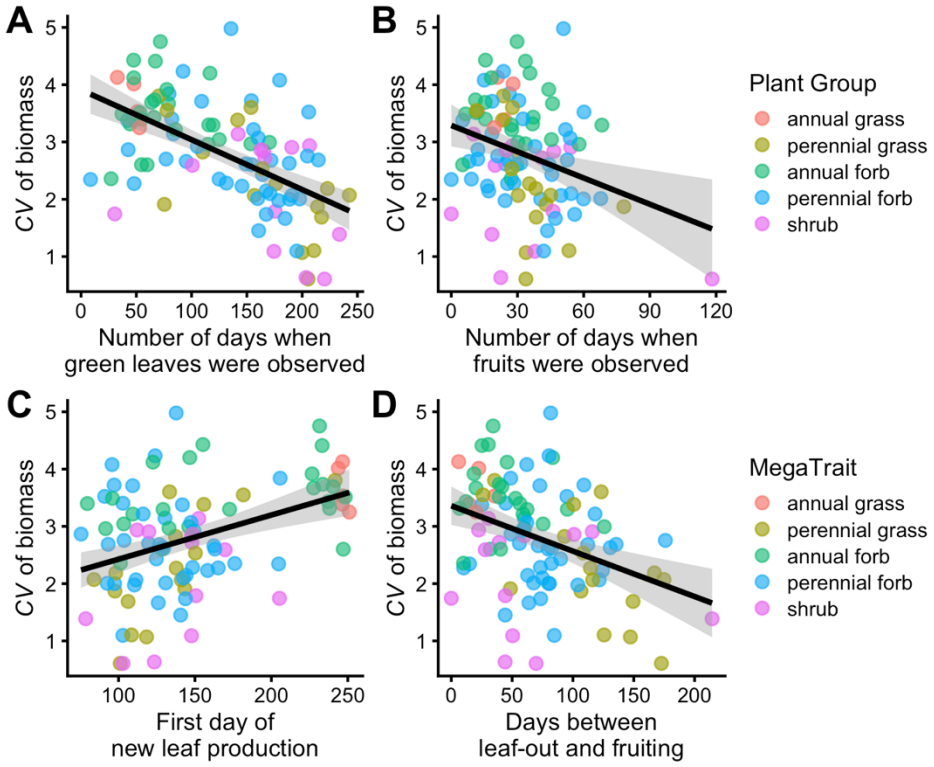

Figure 3.1. Phenological traits predict population stability for 98 dryland plant species including (A) first day of new leaf production, (B) number of days annually when green leaves were observed, (C) number of days between leaf-out and fruit onset, and (D) number of days annually when fruits were observed. Each point represents the mean value of population stability and phenological trait for a single species. Lines are all significant linear fits and gray bands are 95% confidence intervals around the parameter estimate for the slope. Nonlinear fits (e.g., quadratic) did not improve model fit in any case (*results not shown*).

Plant species with more stable population abundance additionally had a greater proportion of years in which they grew but failed to fruit. That is, there were no observations of fruit production despite the fact that a species produced new green leaves in at least two months of the year (Fig. 3.2A, $F_{1,95} = 12.18$, $R^2 = 0.11$, $P = 0.0007$). The number of days species maintained green leaves each year was strongly, positively correlated with the number of days species spent fruiting each year ($F_{1,161} = 87.97$, $R^2 = 0.35$, $P < 0.0001$). However, plant species with longer vegetative phenophases also had a greater proportion of years in which they grew but failed to fruit ($F_{1,189} = 197.8$, $R^2 = 0.51$, $P < 0.0001$), suggesting a growth-reproduction trade-off.

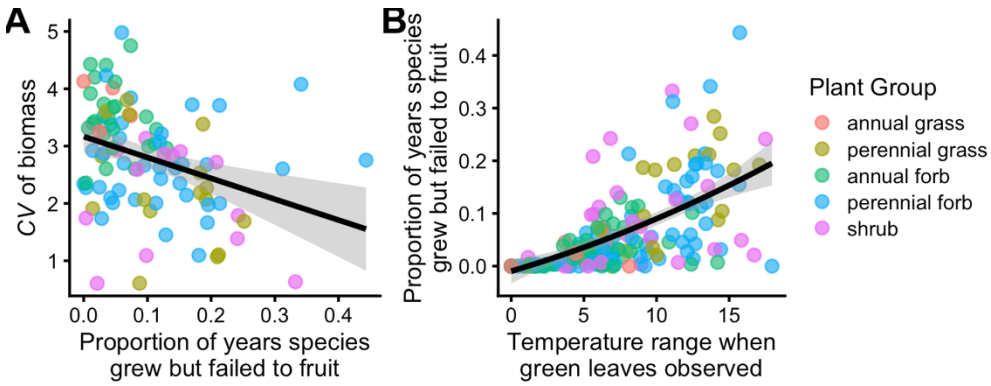

Figure 3.2. Relationship between (A) population stability against failure to fruit and (B) failure to fruit against the temperature range (°C) during green leaf production and maintenance. Each point represents the mean value of each variable for a single plant species. Lines are linear fits and gray bands are 95% confidence intervals around the parameter estimate for the slope.

Among the phenological traits we examined, leaf duration, estimated by the average number of days per year when green leaves were produced (Fig. 3.1A) was the best predictor of population stability based on model selection procedures. This conclusion was supported by the large delta *AICc* (= 28.7) against the next best phenological predictor, which was the average number of days between leaf-out and fruit onset (Fig. 3.1D). These two traits were also the best predictors of average population abundance across the time

series (Supplemental Appendix B, Fig. B3), and thus are also indicators of species commonness on the commonness-rarity spectrum.

3.3.2 Phenology - population stability relationships were independent of phylogenetic relatedness

We found no significant phylogenetic signal (Pagel's λ) in our metric of temporal stability (*CV* of biannual biomass, λ = 0.00007, logL(λ) = -103.7, $P > 0.99$). Likewise, phenological traits also lacked significant phylogenetic signal, including leaf duration, day of leaf onset, days between leaf-out and fruiting, and fruit duration (all $P > 0.99$).

The direction and significance of correlations between the phenological traits and population stability were similar in analyses that accounted for species evolutionary histories using phylogenetic independent contrasts *(PIC*s). The most predictive phenological trait, the duration of green leaf production still ranked first in *PIC*s ($F_{1,77}$ = 24.37, $R^2 = 0.24$, $P < 0.0001$, delta *AICc* = 5.17), and the next best predictor was the average number of days between leaf-out and fruit onset. Full results for phylogenetically corrected analyses are presented in the Supplemental Appendix B.

3.3.3 Climate drivers of phenological traits in dryland plant species

Phenological traits were correlated with climate variables (Supplemental Appendix B, Fig. B4). The duration of active leaf growth was best predicted by the temperature range experienced during the vegetative phenophase ($F_{1,189}$ = 881.8, R^2 = 0.82, $P < 0.0001$). Species that waited until later in the year to begin growing then produced leaves when minimum temperatures were warmer ($F_{1,189} = 57.41$, $R^2 = 0.23$, $P < 0.0001$), and conditions

were wetter ($F_{1,189}$ = 211.6, R^2 = 0.53, P < 0.0001), but their populations showed more temporal instability (Fig. 3.2C). Populations with a larger proportion of failure-to-fruit years maintained green leaves throughout a larger range of temperature conditions (Fig. 3.2B, $F_{1,191}$ = 122.4, R^2 = 0.391, P < 0.0001).

Species that maintained green leaves for more days of the year, species that waited longer to fruit after leaf-out, and species that failed to fruit more frequently were all associated with similar climatic variables. They experienced lower minimum temperatures (R^2 = 0.19, 0.25, and 0.10, respectively; all P < 0.0001), higher maximum temperatures (R^2 = 0.28, 0.08, and 0.12, respectively; all P < 0.0001), a subsequent broader range of temperatures (R^2 = 0.82, 0.48, and 0.39, respectively; all P < 0.0001), and began initial leaf production in drier conditions (R^2 = 0.17, 0.23, and 0.09, respectively; all P < 0.0001).

3.4 Discussion

Phenological traits were strong predictors of temporal stability in population abundance in characteristic grassland and shrubland ecosystems of the Chihuahuan Desert of North America. Plant species with long vegetative and reproductive phenophases had greater population stability than species with shorter phenophases. Compared to prior studies which have evaluated traits as predictors of population stability in plants, the strengths of the relationships reported here exceeded those using phenotypic or allocation traits, such as the leaf economic spectrum (Májeková et al. 2014). Phenological traits in our study explained differences in population stability similarly to the physiological traits (specific leaf area, foliar nitrogen, and water use efficiency) that explained “booms” in population fecundity in a desert annual plant community in the Sonoran Desert (Angert et

al. 2009). Our work revealed novel, phenological predictors of population stability that could be useful to explore in other ecosystems and organisms.

We put forth two alternative hypotheses linking phenological traits with population stability: (1) Species with longer phenophases have more stable temporal dynamics because they can withstand a broad range of environmental conditions. (2) Species with longer phenophases are less temporally stable because individuals face greater risk of infrequent extreme events. Our analyses strongly supported the first hypothesis. The single best predictor of population stability was leaf duration, estimated by the average number of days per year when green leaves were produced (Fig. 3.1A). In fact, leaf duration explained approximately 35% of the variation among species in their population temporal stability.

Phenological traits, including both the onset date and duration of phenophases, were tightly coupled to climate variables. In particular, plant species that waited until later in the year to begin growing, produced leaves under warmer, wetter conditions. Previous studies have associated this acquisitive strategy with the ability to quickly respond to rainfall events. Plant species with this strategy tend to have faster resource acquisition and faster growth and germination rates (Lasky et al. 2016). In contrast, species that maintained green leaves for more days of the year, species that waited longer to fruit after leaf-out, and species that failed to fruit more frequently were all associated with similar climatic variables. These plants experienced lower minimum temperatures, higher maximum temperatures, subsequently a broader range of temperatures, and began initial leaf production under drier conditions, on average. These more conservative phenological traits are commonly associated with species that can withstand drought conditions, store or better

access available water, and have slower rates of growth (Lasky et al. 2016). While trade-offs between allocation to vegetative growth versus reproduction occur commonly across the tree of life (Stearns 1992, Hulshof et al. 2012, Silvertown et al. 2015), we found mixed support for this trade-off. Species that maintained green leaves for more days of the year also tended to fruit for a longer time period, even if they did fail to fruit more frequently.

As climates worldwide are getting hotter and more variable (IPCC 2013), phenological traits and phenological changes may be particularly informative of future destabilization of population abundance. Phenological strategies may make some species more vulnerable to a changing climate. Previous meta-analyses have found that species that begin growing earlier in the year are most sensitive to changing climate, although most of the evidence comes from temperate, not dryland, biomes (Pau et al. 2011, Wolkovich et al. 2012). Growing earlier in the year can put species at risk of frost damage (Inouye 2008), and many dryland species are cold-intolerant (Pockman and Sperry 1997), leading to drastic responses to extreme freeze events (Medeiros and Pockman 2011, Ladwig et al. 2019). However, decreased water availability throughout the year is certain to become the most urgent, consistent pressure in dryland regions. In the arid Southwestern U.S., this pressure will intensify with ongoing delays in the monsoon rainy season towards later in the year (Grantz et al. 2007, Cook and Seager 2013). In this region, the majority of plant growth occurs in response to monsoon rainfall, during which time precipitation not only relieves the stress of summer drought but also provides a degree of cooling via associated cloud cover. We found that the propensity to abandon fruiting increased with the wide range of temperatures a species endures during its growth phase. Therefore, we predict that the most stable populations under future climate conditions will be those that grow over a

long window and do not fruit regularly. Species with slow, conservative growth rates spanning long time windows may gain from increased water use efficiency, and those that save resources for infrequent reproduction may increase net fitness by avoiding costs of reproduction during years with low resource availability (Angert et al. 2007, Venable 2007).

In climatically stochastic environments, such as drylands, sustaining perennial vegetation and reproductive structures can be successful strategies, but still expose plants to a wider range of environmental extremes than species with narrow phenophases. Similar to prior work, we found that species with earlier leaf-out dates were exposed to colder temperatures (Polgar and Primack 2011, Richardson et al. 2018). Species that maintain green leaves for more days annually, did so through a broader range of temperatures. This growth strategy could, for example, put individuals at risk of summer drought (Barber et al. 2000) or allow them to capitalize on growth opportunities in the cooler, 'shoulder seasons' of each year (Petrie et al. 2015a). Longer growing seasons require maintenance of perennial structures through drier conditions, which could limit net carbon gain or even cause net carbon losses (White and Nemani 2003, Han et al. 2018). Similarly, species with broad reproductive windows can experience more failure to fruit, at least among some genotypes (Thomson 2010). However, even though these strategies were not without risk, the phenological traits of early onset and longer phenophases were both associated with higher temporal stability in population abundance.

Although we were able to capture a large range of trait variation among species, our study was limited by some practical factors. Firstly, the monthly frequency of phenology observations likely missed some changes in phenology over the study period.

The advancement of most phenological transition dates is on the order of 2-10 days per decade (Wolkovich et al. 2012). Thus, our monthly sampling frequency would not capture changes on this scale. We also recorded the phenology of up to ten representative individuals on each observation date, which can bias observations toward individuals in the most advanced phenological stages. This methodology likely discounts cryptic variation in phenology within individuals or among individuals in a population (Albert et al. 2019). We defined the onset or offset date of a phenophase as the date when at least 25% of the population entered or exited a phenophase. A gaussian distribution describing the probability of entering or exiting that phenophase may be more useful, but easier to develop for some species than others, depending on population size and variability. Future analyses could incorporate more process-based metrics (those that incorporate variability in the population and within years) rather than transition dates (Inouye et al. 2019).

Long-term monitoring programs are uniquely poised to capture ecologically meaningful trait data (Kominoski et al. 2018). Our analyses leveraged decades of population monitoring data made across different biomes and variable climate conditions to estimate both long-term population stability and population-mean phenological traits. These metrics can be difficult and time consuming to measure, especially in stochastic environments. Therefore, our results demonstrate the importance of long-term data for advancing ecological understanding of population dynamics and stability, an understanding that cannot be easily replaced by space-for-time substitution (Gerst et al. 2016, Harris et al. 2018, Kazenel et al. 2019).

We revealed exciting potential for phenological traits to explain differences in population dynamics among species. We found that simple phenological traits were strong

predictors of population stability measured across multiple decades in highly stochastic environments. These traits link life-history strategies in vegetative and reproductive investment to underlying climatic presses and pulses. While much attention has been given to how phenology is changing in a warming and more variable climate, further study of how phenological traits cause population instability will improve understanding of which species, and which life history strategies, are most sensitive to seasonal shifts in precipitation and temperature.

3.5 Supplemental Appendix B

Comparing metrics of population stability

In our dryland study sites, some species grow very briefly in either the spring or monsoon growing seasons. Among the 98 species we included in our study, 19 species maintained green leaves for less than 60 days per year, on average. Because of this, some studies report the maximum seasonal biomass, either spring or monsoon biomass, as a single metric of annual biomass. If these species always have zero biomass in one season our calculation of CV may result in an inflated estimate of biomass variability. However, reducing our biomass dataset to one annual measurement of productivity from two could reduce our statistical power by half. Therefore, we compared biannual *CV* values to the *CV* of maximum annual biomass. These values were very highly correlated ($F_{1,92}$ = 1893, R^2 = 0.95, $P < 0.0001$). We also compared the relationship between these two metrics of *CV* to phenological traits and found that they performed similarly. For example, the relationship between the *CV* of maximum annual biomass and leaf duration was still significantly positive ($F_{1,92}$ = 39.16, R^2 = 0.30, $P < 0.0001$), showing us that our trends weren't skewed

by the presence of many short-lived, seasonal specialist species. Based on these results, we chose to report the biannual *CV*, the metric with the larger sample size.

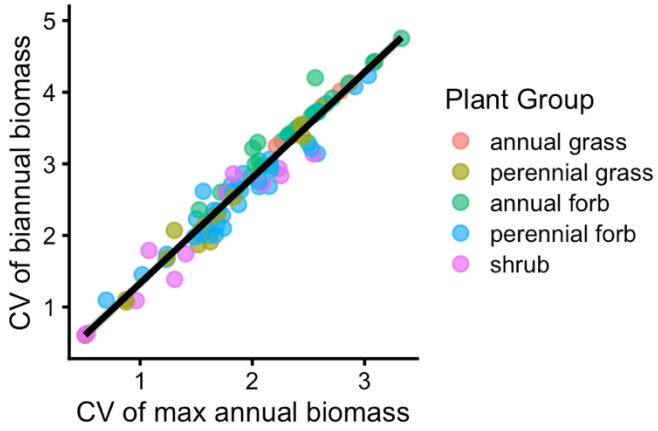

Supplemental Figure B1. CV of maximum annual biomass compared to the CV of biannual biomass. Each point represents the average population stability values of a species and line represents a linear fit.

Accounting for phylogenetic relatedness

Our analysis treats each species as an independent unit. However, the evolutionary histories of species mean that species are not statistically independent, particularly when traits have strong phylogenetic signal. We assessed whether phylogenetic non-independence altered our conclusions by both assessing phylogenetic signal in species phenological traits and stability metrics and using phylogenetically corrected regression analysis with phylogenetically independent contrasts (*PIC*s) (Garland et al. 1992). Of the 98 species in our original analysis, 80 were present in a time-calibrated plant phylogeny built with 31,383-species by Qian and Jin (2016), that we pruned to our focal species.

We tested whether there was a phylogenetic signal (Pagel's λ) in the *CV* of biannual biomass, and there was no significant signal, indicating that differences in *CV* of biomass

among species was not significantly driven by phylogenetic relatedness (λ = 0.00007, logL(λ) = -103.7, $P > 0.99$). Likewise, there was no significant phylogenetic signal in the phenological traits of leaf duration ($P > 0.99$), day of leaf onset ($P > 0.99$), days between leaf-out and fruiting ($P > 0.99$), and fruit duration ($P > 0.99$).

We compared the strongest correlations between population stability and phenological traits using the phylogenetic independent contrasts (*PIC*s) as our units of replication, rather than the species (the tips of phylogenetic trees). The direction and significance of all relationships remained similar. There was a positive relationship between CV of biomass and the day of leaf-out for *PIC*s ($F_{1,77}$ = 17.95, R^2 = 0.19, $P <$ 0.0001). There was a negative relationship between CV of biomass and the duration of green leaf production and maintenance for *PIC*s ($F_{1,77}$ = 24.37, R^2 = 0.24, $P < 0.0001$). Model comparisons still showed that leaf duration was the best predictor of population stability, slightly trailing the day of leaf-out (delta *AICc* = 5.17). There was a negative relationship between CV of biomass and the number of days between leaf-out and fruiting for *PIC*s ($F_{1,77}$ = 5.09, R^2 = 0.06, P = 0.03). There was a negative relationship between CV of biomass and the duration of fruiting for *PIC*s ($F_{1,77}$ = 9.44, R^2 = 0.11, P = 0.003).

Relatedness of phenological traits

Many phenological traits were correlated to one another.

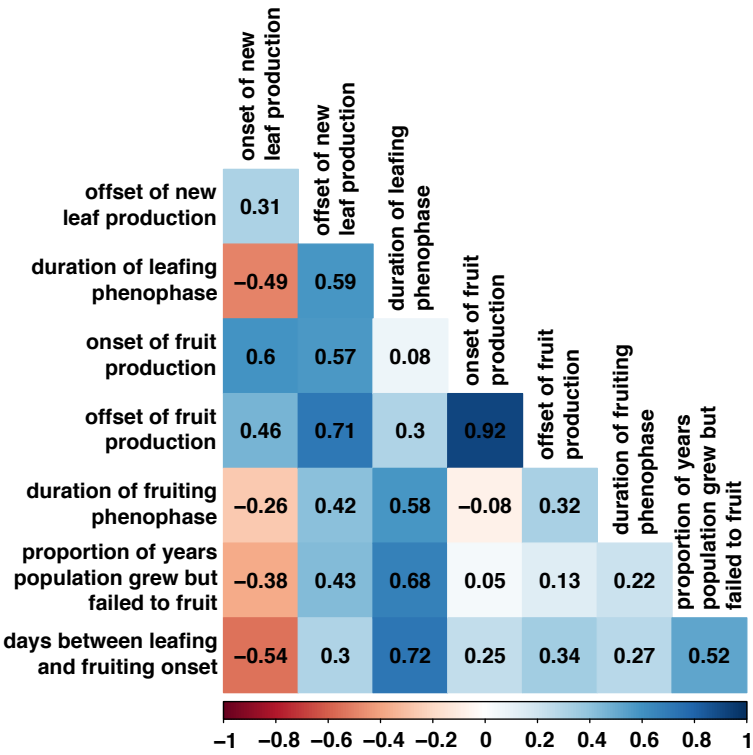

Supplemental Figure B2. Correlogram of all phenological traits included in our analyses. Values represent correlation coefficients (*R*). Darker colors correspond to stronger relationships, with warmer tones indicating negative correlations and cooler tones indicating positive relationships.

Relationships between phenological traits and climate variables.

Phenological traits were correlated with both temperature and precipitation climate variables. Specifically, the duration of active leaf growth was best predicted by the temperature range experienced during the vegetative phenophase ($F_{1,189} = 881.8$, $R^2 = 0.82$, $P < 0.0001$). Species that waited until later in the year to begin growing produced leaves when minimum temperatures were warmer ($F_{1,189} = 57.41$, $R^2 = 0.23$, $P < 0.0001$), and conditions were wetter ($F_{1,189} = 211.6$, $R^2 = 0.53$, $P < 0.0001$), but their populations showed more temporal instability (Fig. 3.2C). Populations with a larger proportion of failure-to-fruit years maintained green leaves throughout a larger range of temperature conditions (Fig. 3.2B, $F_{1,191} = 122.4$, $R^2 = 0.391$, $P < 0.0001$).

Species that maintained green leaves for more days of the year, species that waited longer to fruit after leaf-out, and species that failed to fruit more frequently were all associated with similar climatic variables. They experienced lower minimum temperatures (R^2 = 0.19, 0.25, and 0.10, respectively; all $P < 0.0001$), higher maximum temperatures (R^2 = 0.28, 0.08, and 0.12, respectively; all $P < 0.0001$), a subsequent broader range of temperatures (R^2 = 0.82, 0.48, and 0.39, respectively; all $P < 0.0001$), and began initial leaf production in drier conditions (R^2 = 0.17, 0.23, and 0.09, respectively; all $P < 0.0001$).

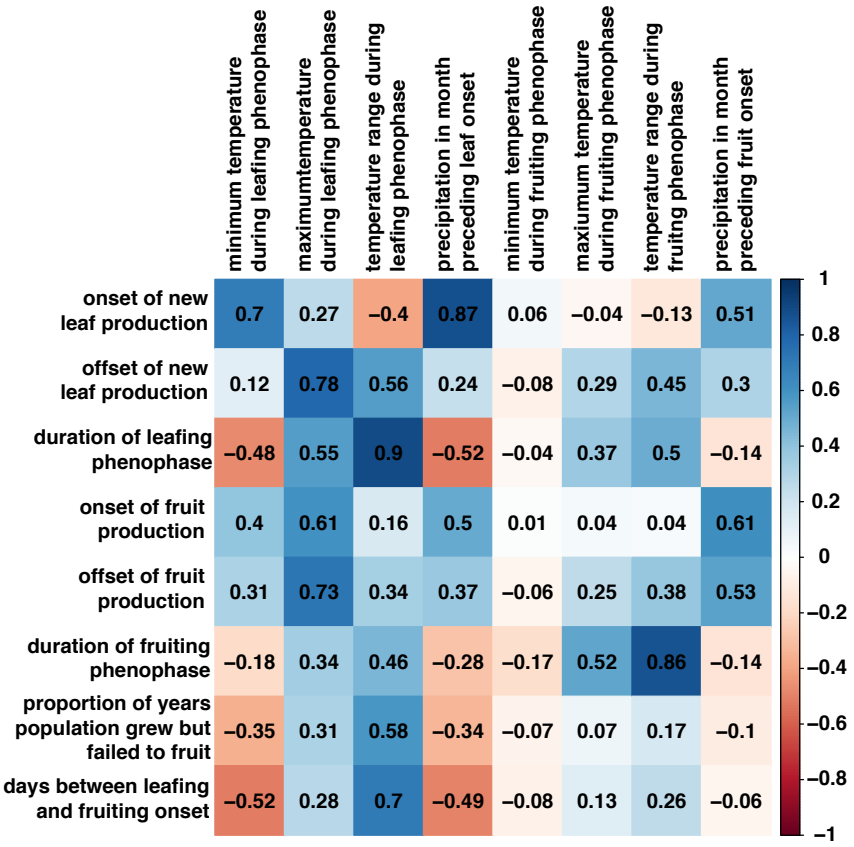

Supplemental Figure B3. Correlogram of phenological traits related to climate variables. Values represent correlation coefficients (R). Darker colors correspond to stronger relationships, with warmer tones indicating negative correlations and cooler tones indicating positive relationships.

Phenological traits predicted plant population size

The most abundant species on the landscape maintained green leaves throughout the year. The most abundant species also failed to fruit in more years, indicating that constant investment in vegetative structures results in a reproductive cost.

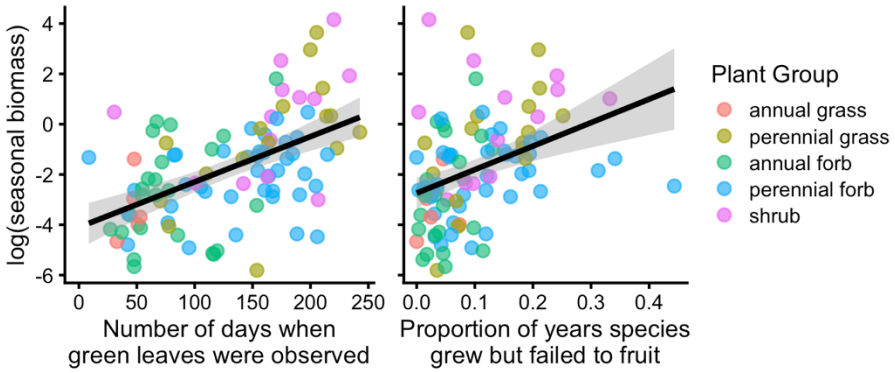

Supplemental Figure B4. Phenological traits predict population size for 98 dryland plant species including (A) number of days annually when green leaves were observed and (B) the proportion of years in which species grew but failed to produce fruit. Each point represents the mean value of population stability and phenological trait for a single species. Lines are linear fits and gray bands are 95% confidence intervals around the parameter estimate for the slope. A nonlinear fit (e.g., quadratic) did not improve model fit (results not shown).

Chapter 4

Watching Plants Dance: movements of live and dead branches are linked to atmospheric water demand

Authors: Alesia J. Hallmark[1], Gregory E. Maurer[1,2], Robert E. Pangle[1], Marcy E. Litvak[1]

[1] University of New Mexico, Department of Biology, Albuquerque, NM

[2] Jornada Basin LTER Program, New Mexico State University, Las Cruces, NM

4.1 Introduction

Although movements of vegetative and reproductive plant organs are well-documented (Darwin and Darwin 1880), diurnal movements of woody branches have only recently been described in detail (Puttonen et al. 2016, Zlinszky et al. 2017). There is mounting evidence that branch movements may occur in many woody species, but previous studies only document movements in greenhouse conditions (Puttonen et al., 2016; Zlinszky et al., 2017), and over short time frames. It is unclear how frequently this phenomenon occurs in nature, whether movement patterns persist across long time periods, what the potential drivers of branch movements may be, and what role these movements may play, if any, in organismal to ecosystem feedbacks.

Canopy size, shape, branching architecture, and orientation influence plant physiological processes and interactions with other organisms and the environment (Norman and Campbell 1989). In particular, the architecture of branches and leaves affects light penetration, self-shading, transpiration rates, rainfall interception, stemflow and plant

microclimate (Valladares and Pugnaire 1999, Falster and Westoby 2003, Iida et al. 2005, Niinemets 2010). Because woody canopy shape, size, and architecture affects so many facets of plants, daily or sub-daily branch movements have the potential to continuously modify plant-organismal and plant-environmental interactions.

Changes in environmental conditions can trigger a range of non-woody plant movements. Daily cycles of light can elicit movements of leaves and flowers, using mechanisms such as changes in turgor pressure, circadian hormonal signaling and gene expression, and asymmetric growth or cell expansion (Atamian et al. 2016, Apelt et al. 2017). The consequences of light-induced movements range from reduced photoinhibition or herbivore damage to increased light interception or pollinator visitation (van Doorn and van Meeteren 2003). Leaves can also move rapidly in response to temperature changes, often to shelter delicate tissues from extreme heat or cold, enhance photosynthetic uptake, or increase water conservation (Smith 1974, Ludlow and Björkman 1984, Comstock and Mahall 1985, Gamon and Pearcy 1989, Nilsen 1991). Differences in stem and leaf water potential can drive or enhance leaf movements, altering rates of photosynthesis, stomatal conductance, and photoinhibition (Nilsen 1987, Kao and Forseth 1992, Xu et al. 2009). The mechanisms of non-woody movements vary widely between species and only a fraction of these mechanisms may be realized in woody tissues, especially dead wood.

Existing sensor networks can be leveraged to explore the connections between branch movements and environmental conditions across a wide range of ecosystems. In two previous studies of rapid branch movements, researchers used high resolution terrestrial laser scanning (TLS) to track overnight branch movements in two European silver birch (*Betula pendula*) trees (Puttonen et al. 2016) and nocturnal movement patterns

in several other tree species growing in greenhouse conditions (Zlinszky et al. 2017). Although their techniques yielded extraordinarily detailed point clouds, TLS equipment can be expensive, datasets prohibitively large, and analyses computationally intensive. Visible-spectrum cameras provide a cheap, easy-to-use alternative to monitoring branch movements. Research networks such as PhenoCam, EuroCam, and AUSCam have accumulated years of time series imagery. Cameras in these networks collect repeat imagery of static scenes, often at hourly frequency. They have been installed in natural, experimental, agricultural, laboratory, greenhouse, and urban environments (Richardson et al. 2007, Nichols et al. 2013, Petach et al. 2014). Although repeat digital photography has most often been used to relate canopy reflectance to carbon uptake and phenological transition dates (e.g. leaf-out and senescence), multiple studies have tracked leaf movements using photographic techniques that could be translated to branch monitoring (Biskup et al. 2007). Many cameras have been co-located with meteorological, soil, and stem sensor networks, data from which could be coupled with observations of diurnal branch movements.

To better characterize the occurrence and potential consequences of branch movements in woody species, we first present a survey of near-surface repeat digital photographs from the PhenoCam network. We then focus on one species in particular, the desert shrub creosote (*Larrea tridentata*) to 1) quantify branch movements in both live and dead branches, 2) identify the potential abiotic and/or biotic drivers of these movements, and 3) discuss potential plant-environmental feedbacks of these movements. We address these goals across a range of environmental conditions and across daily to seasonal time scales. The small stature, canopy structure, and dramatic branch movements of creosote

made images of this species particularly easy to analyze. In addition, the extreme variability of semi-arid environments in which creosote lives provided a greater range of conditions under which to study the triggers and ramifications of branch movements. We hypothesized that 1) dead branches would be more sensitive to changes in atmospheric moisture and temperature while live branch movements would be more sensitive to changes in stem water potential and atmospheric demand, and 2) branch movements would affect plant microclimate, namely soil temperature.

4.2 Methods

4.2.1 Cross-site survey of woody plant movements

We surveyed PhenoCam imagery from cameras installed at NEON (National Ecological Observatory Network) sites. Over the past decade, NEON sites have been established to represent a variety of biomes, species, and environmental conditions (Keller et al. 2008). PhenoCams at these sites are placed to capture canopy, understory, and streamside images, providing a range of angles from which to potentially view branch movements (Elmendorf et al. 2016). NEON PhenoCams take up to 4 images per hour, increasing the probability of capturing fast branch movements. Special attention was paid to imagery from around dawn and dusk and during both humid and dry time periods. Unfortunately, camera position and rate of image capture made assessing branch movements at some sites impossible, thus, this survey simply highlights the diversity of species and ecological contexts in which branch movements can be observed. Lack of inclusion does not indicate a lack of branch movement at a given site, only that we did not detect movements in the images surveyed, during the time periods we surveyed. We

attempted to identify live and seemingly dead branches, including fallen logs, within each camera scene.

4.2.2 Case study: branch movements in creosote

4.2.2.1 Site description

We more extensively documented branch movements at a creosote shrubland within the Sevilleta National Wildlife Refuge and Long-Term Ecological Research site in central New Mexico, USA (34.334944 N, -106.744167 W). This study site has been operational since 2007 and has been an Ameriflux core site (US-Ses) since 2013 (D'Odorico et al. 2010a, He et al. 2010, Anderson-Teixeira et al. 2011a, Petrie et al. 2015b). The vegetation at the site is dominated by creosote (*Larrea tridentata*), with sparse grasses (*Bouteloua* spp., *Pleuraphis jamesii*, and *Scleropogon brevifolius*), scattered forbs (*Machaeranthera pinnatifida*, *Townsendia annua*, and *Gutierrezia sarothrae*), and cacti (*Opuntia macrocentra*).

All data for our study of creosote branch movements were collected between July 31, 2015 and December 5, 2015. This study period encompassed a range of abiotic conditions. The growing season in this area of the northern Chihuahuan Desert is bimodal, with a short growing season in the spring (March-April) followed by a hot and dry period (typically May-June), and the main growing season occurring from mid-July to early October. The first half of our study period encompassed the main growing season (July 31-September). During this time, the average air temperature was 23.2°C ± 4.7°C s.d. and the median volumetric soil water content was 9.7% ± 0.5% s.d. During the last half of the study period (October-December), the growing season gave way to a wet winter, with the average

air temperatures dropping to 9.8°C ± 7.0°C s.d. and the median volumetric soil water content rising to 15.9% ± 3.3% s.d.

In February 2011, nearly five years before our study, this site experienced an extreme cold event, with temperatures dropping to -30°C. Although many shrubs suffered >90% canopy dieback, there was very little creosote mortality (Ladwig et al. 2019). In the ensuing years, shrub canopies regrew from the base of each plant, leaving a unique crown of dead branches. All dead creosote branches described in this study remain connected to the central stem of the plant, where the living branches also originate, but are visibly distinct from their living counterparts. They have no vegetative growth or living tissue from the stem tip to the stem base where the branch enters the soil. Dead branches are dry, brittle, missing most or all of their bark, have deep cracks, and have no measurable xylem water.

4.2.2.2 Repeat digital photographs

Three Moultrie Game Spy I-60 cameras (EBSCO Industries, Inc., Birmingham, AL, USA) were positioned to photograph creosote shrubs within 5 meters of the main site instrumentation. Photos were taken hourly throughout the study period. Infrared camera flashes illuminated each scene at night. Within each scene, we selected multiple branch points (branch tips or nodes) which could be distinguished in photos throughout the study period and were visible during both day and nighttime conditions. Additionally, we placed white plastic balls on several branches so that their position could be more easily tracked. Branches ranged from 0.9-1.4 m in total length from 11 individual shrubs. All scenes and tracked branches are shown in Supplemental Figure C1.

Branch movements were quantified by recording the *x*- and *y*-coordinate of branch points within each hourly photo. Branches flexed along their entire length, bending in *x*, *y*, and *z* coordinate space. This constantly changing branch geometry, as well as the density of branches at the base of the shrub, made it impossible to track the trajectory of entire branch lengths in still photographs. Our analysis focused on changes in each branch point's vertical (*y*-coordinate) position within each photo time series, although this number only partially quantifies the dramatic movement these branches display. To standardize this measurement for branches of different lengths and at different distances from the camera, we z-scored the *y*-coordinate time series of each branch point, a metric we call *Branch Position*. Positive Branch Position indicates that a branch is oriented more skyward while negative Branch Position indicates that a branch is closer to the ground. A larger absolute value of Branch Position indicates that the branch moved further from its average vertical position. We visually assessed live branches to confirm that branch growth was minimal over the course of the study period. Stationary objects were tracked within each scene to detect wind interference and ensure that cameras did not drift significantly over the course of the study period. We removed outlier Branch Position points (<0.01% of data), filled gaps of less than 6 hours using a spline method, and smoothed all data to decrease noise.

4.2.2.3 Meteorological data

We measured relative humidity and air temperature with an HMP45C Vaisala temperature/relative humidity probe (Vaisala Instruments, Helsinki, Finland) and used these values to calculate vapor pressure deficit. Incoming photosynthetically active radiation was measured with a Kipp & Zonen LI-190 PAR sensor (LICOR, Lincoln, NE,

USA). These sensor data were continuously measured at 10Hz frequency and stored as 30-minute averages. Precipitation, recorded as a 30-minute sum, was measured using a TE525 Texas Electronics 6" tipping bucket rain gage (Texas Electronics, Dallas, TX, USA).

From 7 Aug. 2015 - 15 Aug. 2015, we measured stem water potential using a stem psychrometer installed at the base of a living creosote stem. After 15 Aug. 2015, we installed an automated PSY1 stem psychrometer (ICT International, Armidale, Australia) at the base of a living stem on a different creosote growing approximately 3 m from the first. Stem water potential was calculated as the difference in wet bulb and dry bulb thermocouple temperatures, recorded every 30 minutes, and corrected for ambient air temperature (Dixon and Tyree 1984). All psychrometers were calibrated using standardized saline solutions in the lab before installation.

We measured soil temperature and soil water content in four soil profiles at 2.5, 12.5, 22.5, 37.5, and 52.5 cm depths. Two "covered" profiles were located under creosote canopies and another two "uncovered" profiles were located in bare canopy interspaces without shrub or grass cover. Soil water content was measured with CS-616 water content reflectometers at each profile depth (Campbell Scientific, Logan, UT, USA). Soil temperature was measured with thermocouple probes at each depth (T-107, Campbell Scientific, Logan, UT, USA) and additionally with dielectric water potential sensors at 22.5 and 37.5 cm depths (MPS6, Decagon Devices, Pullman, WA, USA). Soil temperature and water content were measured every 5 minutes and recorded as 30-minute averages. Other variables like air pressure, wind speed, and moon phase were measured and analyzed but are not shown here due to lack of correlation with branch movements.

4.2.2.4 Data processing

Branch points were observed and their *x*- and *y*-coordinates recorded using a custom Matlab script (The MathWorks Inc. 2019). Data manipulation and statistical analyses were conducted with R 3.5.0 (R Core Team 2020). In order to disentangle the relative importance of multiple abiotic factors which all displayed some degree of diurnal periodicity, we calculated cross-correlations between Branch Position and abiotic variables at differing hourly lags (from -3 to +3 hours) using the *ccf*() function from the R package *stats* (R Core Team 2020). Cross-correlation fits were calculated on both daily and seasonal time scales. To assess how well branch movements were correlated with abiotic factors on daily time scales, we calculated lagged correlations within 5-day rolling windows along the entire time series. There was a total of 118 these 5-day windows included in our analysis. Within each 5-day window, the correlation between up to 120 hourly data points per data time series were compared. We also calculated the correlation between abiotic variables and Branch Position across the entire time series, using all hourly data from July-December to fit cross-correlation models. This approach helped us determine whether variables were correlated across the entire study period or only within certain seasons, and whether the lag between the factors changed seasonally.

While multiple environmental variables display diurnal periodicity, we hypothesized that only some have the potential to drive branch movements. This is particularly true for dead branches, which lack the living cells needed to sense sunlight, produce signaling hormones, or create xylem water potential gradients. In order to differentiate between factors that were simply co-correlated with branch movements and those that were correlated and potentially driving branch movements, we assessed the

linear relationship with each abiotic factor at multiple lags. Figure 4.1 illustrates four potential outcomes of this analysis. In each case, there would be a strong, statistically significant correlation between the predictor and response signals. In the first panel, the predictor and response signals are complete synchronized. As the background color of the lower correlation panel indicates, the strongest cross-correlation between the two signals occurs at a 0-hour time lag. The black line in the lower correlation panel shows that the cross-correlation between the two signals is 100%. We may expect to see this signal if the predictor signal elicits an immediate reaction in the response signal. The second panel illustrates a potential scenario when the response consistently lags behind the predictor signal. Here, the strongest cross-correlation between the two signals (averaging ~95% correlation) occurs when the predictor time series is shifted back (earlier) in time. We might expect to see this pattern when the response signal is reacting directly to the predictor variable but takes some time to occur. This scenario *could* occur if the predictor signal was driving the response signal. The third panel illustrates a potential scenario where both signals are highly correlated, but because the response signal consistently leads the so-called-predictor variable in time, the predictor signal *could not be causing* the response signal. Finally, the fourth panel illustrates a scenario where the response signal does not consistently change with the predictor signal over time. We assume this scenario might occur if there is no relationship between the predictor and response signals, or if the predictor signal directly elicits a change in the response signal, but only under certain conditions.

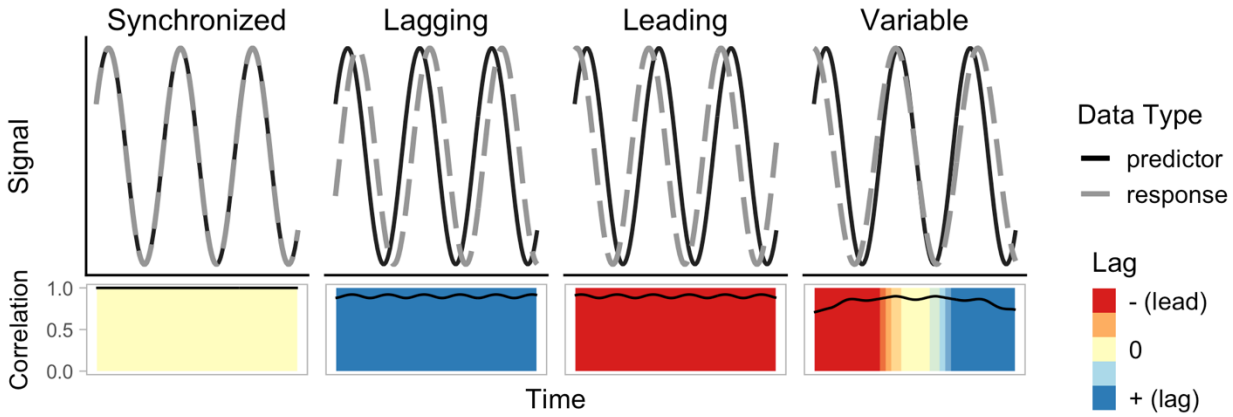

Figure 4.1. Conceptual diagram illustrating four potential outcomes of a lagged correlation analysis. In each scenario, the two time series display similar periodicity and are highly correlated, but the type of lag between the data differs. In the upper panels, the black line represents a potential predictor or explanatory variable, while the grey dashed line represents a response variable. In the bottom correlation panels, the maximum correlation coefficient within a rolling window is illustrated with a black line and the lag at which correlation is optimized is shown by the background color. In the first panel, the two time series are perfectly synchronized, with a correlation of 1 and no time lag between the signals. In the second panel, there is a consistent, positive time lag of the response signal with a high correlation (correlation coefficient nearly equal to 1). In the third panel, there is a consistent, negative time lag (leading effect) of the response signal with a high correlation (correlation coefficient nearly equal to 1). In the fourth panel, the time lag of the response signal varies across the time series, as does the correlation coefficient.

We are using this lagged correlation analysis as a first step in narrowing down the list of possible causal factors related to branch movements. We think this framework is useful when investigating this newly discovered phenomenon in a natural setting where many abiotic and biotic factors display similar diurnal and seasonal periodicity. We emphasize that these analyses do not by themselves indicate direct causation between abiotic drivers and branch movements.

4.3 Results

4.3.1 Cross-site survey of woody plant movements

Using time lapse photography from NEON sites and the PhenoCam Network, we found evidence of diurnal woody branch movements in a range of species and ecosystems, from temperate woodlands to boreal forests and arid shrublands (Table 4.1, Figure 4.2). In some species, we observed live and dead branches moving synchronously, with live and dead branches moving upwards and downwards in tandem. In other species branches moved asynchronously or without discernable diurnal patterns. Humid conditions amplified movements in most species.

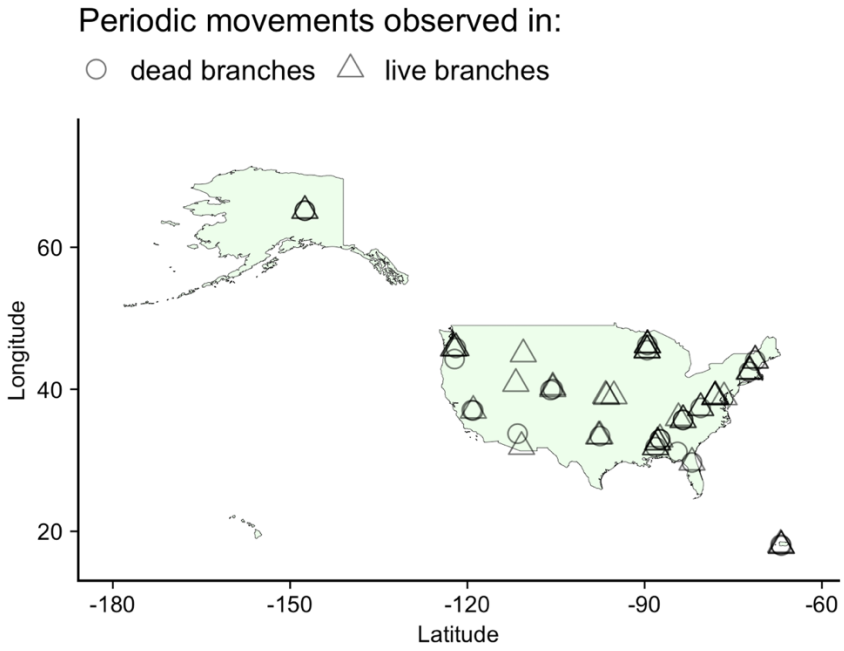

Figure 4.2. Map illustrating the geographic extent of NEON sites where branch movements were observed. Symbols indicate whether live or dead branches were observed moving in each Phenocam scene.

Table 4.1. Site descriptions of NEON PhenoCam locations were branch movements were observed. The NEON Domain, site name, latitude, longitude, and elevation of each site are noted, as well as an indication of whether live or dead branches displayed periodic movements.

NEON Domain	Location	Lat.	Long.	Elev.	Camera Placement	Live Branch Movements	Dead Branch Movements
Northeast	Bartlett Experimental Forest, New Hampshire	44.0639	-71.2874	285	top-of-tower	yes	
	Bartlett Experimental Forest, New Hampshire	44.0639	-71.2874	285	mid-tower	yes	yes
	Harvard Forest, Massachusetts	42.5369	-72.1727	359	top-of-tower	yes	
	Harvard Forest, Massachusetts	42.5369	-72.1727	359	mid-tower	yes	
	Hop Brook, Massachusetts	42.4718	-72.3296	203	stream gauge	yes	yes
Mid-Atlantic	Blandy Experimental Farm, Virginia	39.0337	-78.0418	162	top-of-tower	yes	
	Blandy Experimental Farm, Virginia	39.0337	-78.0418	162	mid-tower	yes	
	Posey Creek, Virgina	38.8933	-78.1468	293	stream gauge	yes	
	Smithsonian Conservation Biology Institute, Virginia	38.8929	-78.1395	364	mid-tower	yes	
	Smithsonian Environmental Research Center	38.8901	-76.5600	30	mid-tower	yes	
Southeast	Flint River, Georgia	31.1854	-84.4374	27	stream gauge		yes
	Ordway-Swisher Biological Station, Florida	29.6893	-81.9934	56	mid-tower	yes	yes
Atlantic Neotropical	Rio Cupeyes, Puerto Rico	18.1135	-66.9868	164	stream gauge	yes	yes
	Guanica Forest, Puerto Rico	17.9696	-66.8687	136	top-of-tower	yes	
	Guanica Forest, Puerto Rico	17.9696	-66.8687	136	mid-tower	yes	yes
Great Lakes	Crampton Lake, Wisconsin	46.2111	-89.4783	518	stream gauge	yes	
	Steigerwaldt Land Services, Wisconsin	45.5089	-89.5864	476	top-of-tower	yes	
	Steigerwaldt Land Services, Wisconsin	45.5089	-89.5864	476	mid-tower	yes	yes
	Treehaven, Wisconsin	45.4937	-89.5857	474	mid-tower	yes	
	UNDERC, Michigan	46.2339	-89.5373	529	top-of-tower	yes	
	UNDERC, Michigan	46.2339	-89.5373	529	mid-tower	yes	yes

Prairie Peninsula	Kings Creek, Kansas	39.1051	-96.6034	339	stream gauge	yes	
	McDiffett Creek	38.9443	-96.4420	376	stream gauge	yes	
	The University of Kansas Field Station, Kansas	39.0404	-95.1922	330	mid-tower	yes	
Appalachians and Cumberland Plateau	Great Smoky Mountains National Park, Tennessee	35.6890	-83.5020	589	top-of-tower	yes	
	Great Smoky Mountains National Park, Tennessee	35.6890	-83.5020	589	mid-tower	yes	yes
	LeConte Creek, Tennessee	35.6904	-83.5038	578	stream gauge		yes
	Mountain Lake Biological Station, Virginia	37.3783	-80.5248	1177	top-of-tower	yes	
	Mountain Lake Biological Station, Virginia	37.3783	-80.5248	1177	mid-tower	yes	yes
	Walker Ranch, TN	35.9595	-84.2804	274	stream gauge	yes	
Ozarks Complex	Black Warrior River, Alabama	32.5415	-87.7982	23	stream gauge	yes	
	Dead Lake, Alabama	32.5417	-87.8039	36	top-of-tower	yes	
	Dead Lake, Alabama	32.5417	-87.8039	36	mid-tower		
	Lenoir Landing, AL	31.8539	-88.1612	10	top-of-tower	yes	
	Lenoir Landing, AL	31.8539	-88.1612	10	mid-tower	yes	
	Mayfield Creek, AL	32.9597	-87.4081	93	stream gauge	yes	yes
	Talladega National Forest, Alabama	32.9505	-87.3933	167	mid-tower		yes
	Tombigbee River, Alabama	31.8534	-88.1589	10	stream gauge		yes
Central Plains	Rocky Mountain National Park CASTNET, Colorado	40.2759	-105.5460	2751	mid-tower	yes	
Southern Plains	LBJ National Grassland, Texas	33.4012	-97.5700	279	mid-tower	yes	yes
	Pringle Creek, Texas	33.3786	-97.7823	255	stream gauge	yes	
Northern Rockies	Yellowstone National Park, Wyoming	44.9535	-110.5391		mid-tower	yes	
Southern Rockies and Colorado Plateau	Como Creek, Colorado	40.0350	-105.5449	3036	stream gauge	yes	yes
	West St Louis Creek, Colorado	39.8914	-105.9154	2920	stream gauge		yes
Desert Southwest	Santa Rita Experimental Range, Arizona	31.9107	-110.8355	999	mid-tower	yes	
	Sycamore Creek, Arizona	33.7491	-111.5069	644	stream gauge		yes

Great Basin	Red Butte Creek, Utah	40.7839	-111.7979	1696	stream gauge	yes	
Pacific Northwest	Abby Road, Washington	45.7624	-122.3303	390	top-of-tower	yes	
	Abby Road, Washington	45.7624	-122.3303	390	mid-tower	yes	
	Martha Creek, Washington	45.7912	-121.9320	354	stream gauge	yes	
	McRae Creek, Oregon	44.2596	-122.1656	880	stream gauge		yes
	Wind River Experimental Forest, Washington	45.8205	-121.9519	368	mid-tower	yes	yes
Pacific Southwest	Upper Big Creek, California	37.0597	-119.2575	1133	stream gauge		yes
	Lower Teakettle, California	37.0058	-119.0060	2149	mid-tower	yes	yes
Taiga	Caribou Creek - Poker Flats Watershed, Alaska	65.1540	-147.5026	233	mid-tower	yes	yes
	Caribou Creek at Poker Flats, Alaska	65.1531	-147.5025	229	stream gauge	yes	yes
	Delta Junction, Alaska	63.8811	-145.7514	529	mid-tower	yes	yes

4.3.2 Case study: branch movements in creosote

At our creosote case study site, we tracked 18 creosote branches in hourly photographs for 126 days between July 31 and December 4, 2015. The end of our study period was cut short by a series of snowstorms that covered the shrubs in snow and fogged the cameras for several weeks. The branches we tracked all displayed cyclical daily movements throughout the entire study period. Using trigonometric methods, we estimate that some branches moved more than 20 vertical centimeters per day during this study period. A timeline and photograph-montage illustrating 48 typical hours of branch movement is shown in Figure 4.3.

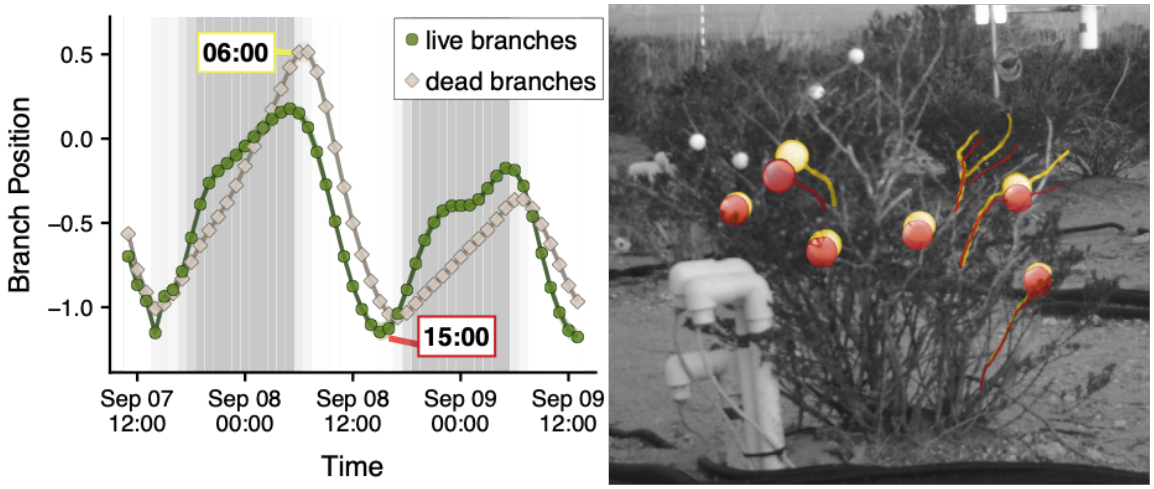

Figure 4.3. Representative daily branch movements. (A) Average hourly Branch Position of live and dead branches across a 48-hr. time period in early September. The background color of the time series represents incoming photosynthetically active radiation, with darker gray bands occurring at night and brightest white midday. (B) A photograph of a shrub taken at 06:00 on 08 Sept. 2019. Ping-pong balls and the branches they are attached to (when visible) are highlighted in yellow. The position of the same ping-pong balls and branches in an image taken at 15:00 that same day are overlaid and highlighted in red.

Creosote branches were typically oriented higher (skyward, steeper angle) at night and lower (groundward, shallower angle) in the day. The most common diurnal pattern of branch movement we observed was downward movement (decrease in branch angle) initiated at dawn, with branches reaching their lowest height midday, and upward movement (increase in branch angle) starting in the afternoon or evening, with maximum height reached just before dawn each day. These diurnal movements were often correlated with the diurnal and weekly-biweekly cycles of relative humidity, air temperature, vapor pressure deficit, and stem water potential (Figure 4.4). Surprisingly, branch movements in creosote did not track seasonal patterns in stem water potential (Figure 4.6). Creosote branches maintained a steeper angle, on average, in the wet winter months than in the hotter monsoon months (Figure 4.5).

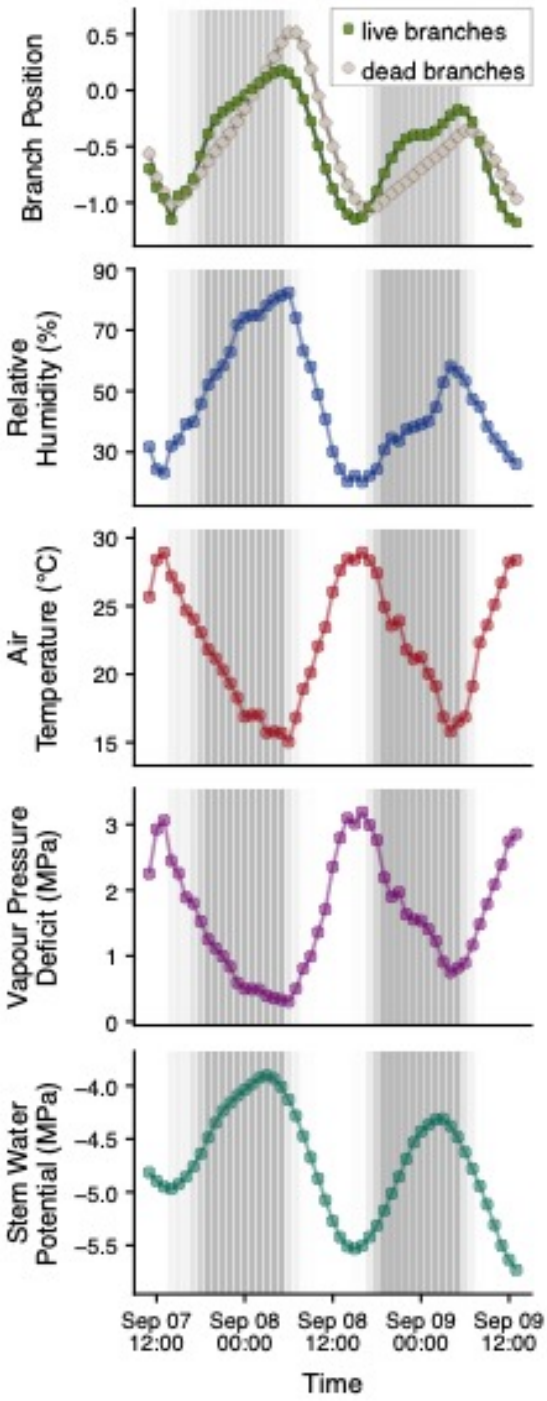

Figure 4.4. Representative daily patterns of branch movement, relative humidity, air temperature, vapor pressure deficit, and stem water potential across a 48-hr. time period in early September. The background color of the time series represents incoming photosynthetically active radiation, with darker gray bands occurring at night and brightest white midday.

4.3.3 Comparing live and dead branch movements

Branch movements of live and dead creosote branches were highly correlated to one another on diurnal and seasonal time scales (Figure 4.5). Live branches, however, consistently moved before dead branches throughout the day. Live branches started to droop earlier at dawn and also stabilized and started raising earlier in the afternoon or evening (Figure 4.4). Over the whole study period, live branches moved, on average, 1 hour before dead branches (Table 4.2). The average cross-correlation coefficient between live and dead Branch Position within all 5-day rolling windows was 84.0% ± 6.1% s.d. and the average time lag was -1.0 ± 0.8 s.d., meaning that live branches changed position ~1 hour before dead branches. When comparing live and dead Branch Position with a single cross-correlation model which included all data from the entire study period, the correlation was 71.9% with a -1.0 hour lag, meaning that live branches changed position an hour before dead branches. Although the average lag between live and branch movements was approximately an hour, we do see a slight change in this lag throughout the study period. In the growing season (July-September), live branches moved 1-2 hours before dead branches (average of all 5-day window correlations = 82.7%, single model correlation = 71.2%) (Figure 4.6). In the winter months (October-December), however, live and dead branch movements were more correlated (average correlation within all 5-day windows = 85.2%, single model correlation = 84.8%) and nearly synchronized (lag decreased to 0-1 hours) (Figure 4.6). Overall, dead branches displayed more extreme ranges of motion than live branches.

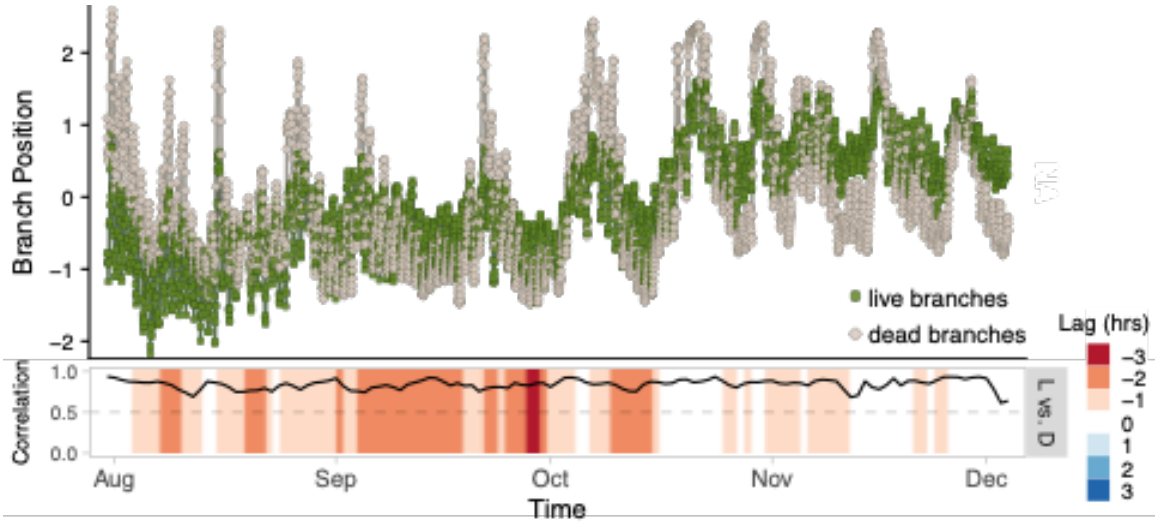

Figure 4.5. Time series of average Branch Position of live and dead branches throughout the study period. Within the lower correlation panel, the black line indicates the maximum correlation between live and dead Branch Position with a 5-day rolling window and the background color of the panel indicates the time lag at which this correlation was maximized. A negative lag indicates that live branch movements precede dead branch movements.

4.3.4 Relationships between Branch Position and abiotic factors

Because dead branches lack leaves, they are often easier to distinguish in photographs. However, their movement patterns often differ in timing or direction when compared to their live, leafy neighbors. In creosote, live branch movements were highly correlated with relative humidity, temperature, vapor pressure deficit, and stem water potential on daily time scales (Figure 4.4, Table 4.2). However, the time lag between live branch movements and these abiotic factors differed throughout the study period (Figure 4.6). Changes in live branch position were in sync or slightly lagging behind (0-1 hour lag) most abiotic factors throughout the growing season and were less consistently correlated with abiotic factors in the winter (Figure 4.6).

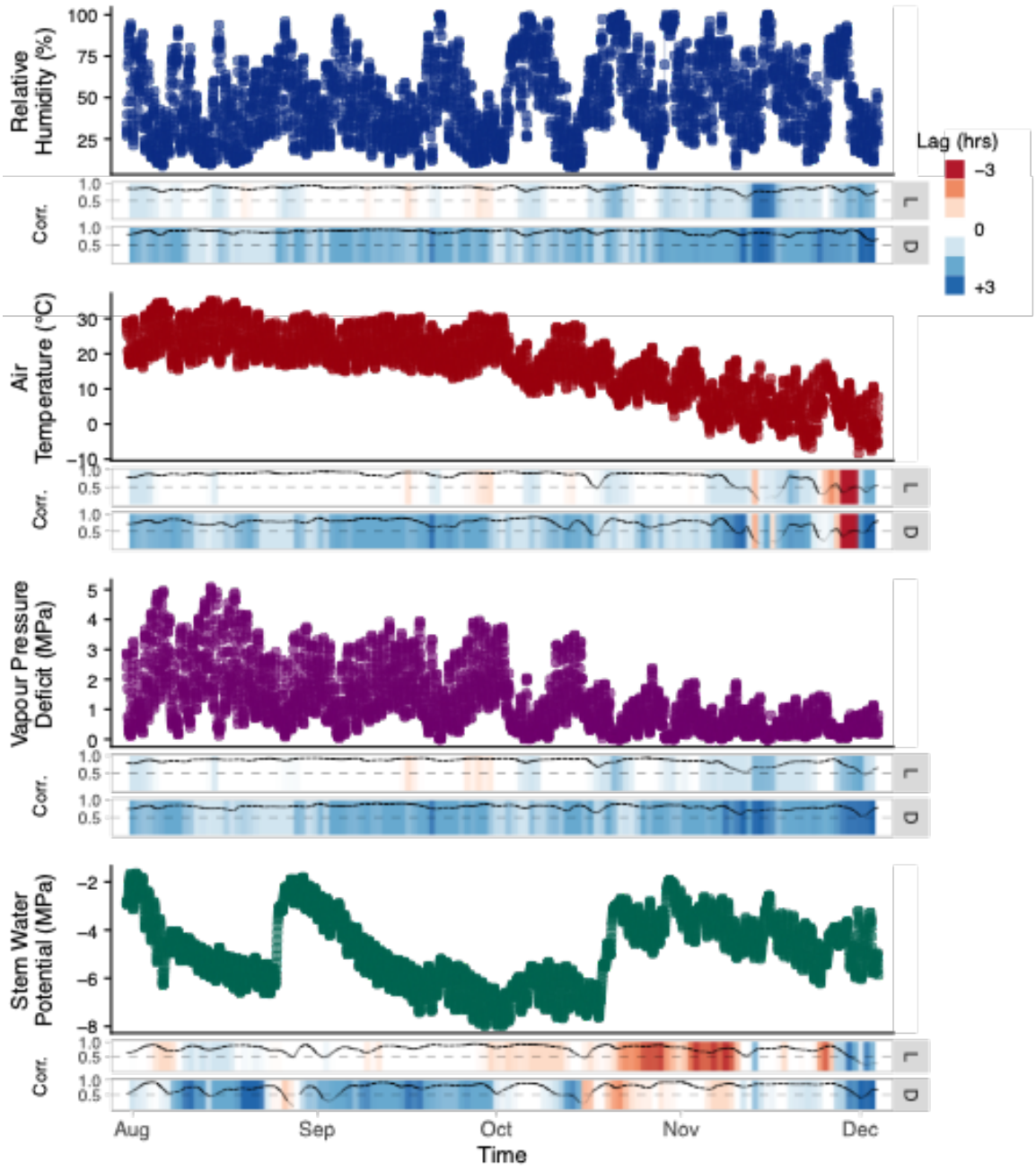

Figure 4.6. Time series of relative humidity, air temperature, vapor pressure deficit, and stem water potential throughout the study period. The correlation plots beneath each time series include a line indicating the correlation between live (facet L) or dead (facet D) Branch Position and the micrometeorological data within a 5-day rolling window throughout the time series. The background color of correlation plots indicates the time lag between branch movements and micrometeorological data, with a negative lag indicating that branch movements precede changes in micrometeorological values.

Within all 5-day windows, Branch Position of live branches was most strongly correlated with relative humidity (85% ± 6%) and vapor pressure deficit (84% ± 10%, moving 0.6 ± 0.7 hours after observed changes in relative humidity and 0.4 ± 0.6 hours after changes in vapor pressure deficit (Table 4.2). In the single, all-season cross-correlation model, however, live branch movements were correlated most strongly with vapor pressure deficit and air temperature (86% with a 0-hour lag and 84% with a 0-hour lag, respectively) (Table 4.2). Notably, live branch movements in creosote were not highly correlated with stem water potential (Table 4.2). In 5-day windows throughout the study period, the -0.3 ± 1.1 hour lag between these two variables indicates on short time scales, live branch movements (measured at or near terminal branch nodes) often occurred *before* changes in stem water potential (measured at the branches base near the ground).

Dead branches consistently moved 1-2 hours after observed changes in relative humidity, air temperature, and vapor pressure deficit throughout the study period (Table 4.2). Stem water potential of live branches and photosynthetically active radiation were also weakly correlated with dead branch movements (Table 4.2). Since the dead branches we tracked have no measurable stem water potential or living cells with which to sense sunlight, we assume this indicates spurious correlations with factors that have similar diurnal periodicity but are not directly causing branch movements.

Table 4.2. Summary of time-lagged correlation results comparing average Branch Position of live and dead branches to potentially causal environmental factors. First, the average correlation coefficient (mean +/- s.d.) within every 5-day rolling window is listed along with the average time lag (mean +/- s.d.) that maximized the correlation between Branch Position and the abiotic variable. Second, we report the correlation coefficient and maximized time lag when all data are used in a single model.

	live branches				**dead branches**			
	all 5-day windows		**all season**		**all 5-day windows**		**all season**	
	correlation	*time lag (hrs)*	*correlation*	*time lag (hrs)*	*correlation*	*time lag (hrs)*	*correlation*	*time lag (hrs)*
relative humidity	85% ± 6%	0.6 ± 0.7	64%	1	88% ± 6%	1.8 ± 0.5	86%	2
vapor pressure deficit	84% ± 10%	0.4 ± 0.6	86%	0	80% ± 7%	1.8 ± 0.5	68%	2
air temperature	79% ± 19%	0.2 ± 0.8	84%	0	71% ± 17%	1.4 ± 1.0	48%	2
stem water potential	75% ± 15%	-0.3 ± 1.1	40%	0	73% ± 17%	1.0 ± 1.2	52%	1
photosynthetically active radiation	68% ± 11%	2.6 ± 0.8	51%	3	47% ± 10%	1.9 ± 1.8	35%	3

4.3.5 Branch Position and soil temperature

We compared creosote Branch Position to changes in soil temperature beneath creosote canopies. Figure 4.7 illustrates the difference between soil temperature under creosote canopies versus soil temperature in unshaded bare ground (ΔT_{soil}) during the months of August and November when soil temperature data were available. Soil temperatures beneath creosote were an average of 1.15°C ± 0.7°C s.d. cooler than in intercanopy spaces in August and 0.21°C ± 0.6°C s.d. in November. There was a diurnal pattern to this temperature difference (Figure 4.7). Soils beneath creosote canopies were slightly warmer than soils in intercanopy spaces right after dawn. During each day, ΔT_{soil} increased, with maximum under-canopy cooling occurring a few hours before sunset. In August, changes in ΔT_{soil} occurred 3.3 ± 0.3 hours after changes in live Branch Position and these factors were fairly well correlated (68% ± 7% average correlation across all 5-

day windows in August). In November, the correlation between live Branch Position and ΔT_{soil} was slightly weaker (57% ± 12%) and the time lag was shorter (0.85 ± 0.37 hours).

In contrast, the average correlation between dead Branch Position and ΔT_{soil} was only 50% ± 14% in August and 45% ± 14% in November. In August, changes in ΔT_{soil} occurring 1.9 ± 0.3 hours after changes in dead Branch Position, but in November changes in dead Branch Position occurred 0.48 ± 0.58 hours *before* changes in ΔT_{soil}.

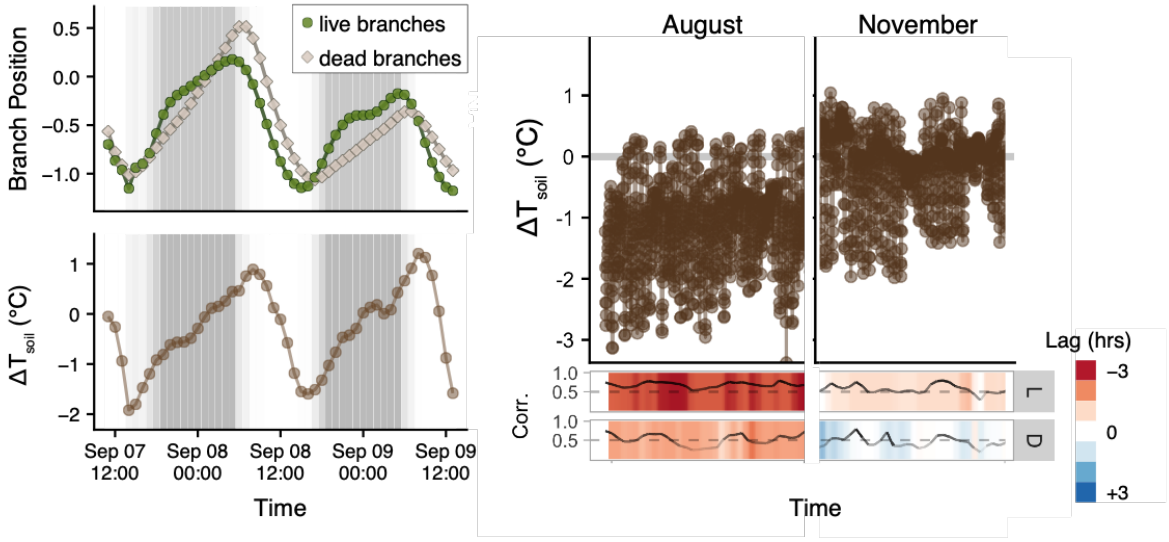

Figure 4.7. ΔT_{soil}, the difference between 2.5cm depth soil temperature under creosote canopies versus soil temperature in unshaded bare ground on daily and monthly time scales. Negative values of soil shading indicate that the soil beneath creosote canopies was cooler than surrounding, unshaded soils. The correlation plots beneath the seasonal time series includes a line indicating the correlation between live (facet L) or dead (facet D) Branch Position and soil shading within a 5-day rolling window throughout the time series. The background color of correlation plots indicates the time lag between branch movements and soil, with a negative lag indicating that branch movements precede changes in soil shading.

4.4 Discussion

4.4.1 Cross-site survey of woody plant movements

We documented diurnal and sub-diurnal branch movements in multiple woody species across a broad range of ecosystems. These observations, along with the findings of

Puttonen et al. (2016) and Zlinszky et al. (2018) show that many species are capable of branch movement that is rapid, quantifiable, and reversible. At least in the case of creosote, these movements seem to occur in response to abiotic conditions, fitting the definition of plant behavior (Karban 2008). Identifying the drivers and repercussions of these movements in different species may be an exciting new field of study, one aided by open-source data and the prevalence of highly instrumented study sites worldwide.

We were able to mine photos from an existing public depository, the PhenoCam network, to retroactively document branch movements across a spectrum of ecosystem monitoring sites (NEON), despite the fact that these cameras were not originally installed for this purpose. Although digital photographs yield lower resolution data than the terrestrial laser scanning techniques employed in previous research, we were able to use them to remotely monitor branch movements across many sites at high frequency (hourly) over long time periods (months to years) as well as readily distinguish live and dead branches. Digital cameras are cheap, easy-to-use, pervasive, and non-invasive instruments with which to study plant movements. Factors such as wind or intense rain can obscure images, but this drawback is common across many sensors, including TLS. Cameras co-located with flux towers, meteorological stations, or other sensor arrays are ideal to further study the relationship between branch movements and abiotic factors.

4.4.2 Case study: branch movements in creosote

We documented branch movements of one species, creosote, over the course of several months. We distinguished subtle differences between live and dead branch movements and leveraged co-located site instrumentation to correlate these movements

with potential abiotic drivers. While gross patterns of movement were the same in all branches – raising skyward at night and drooping groundward in the day – there was a consistent temporal lag between live and dead branches.

Dead branches move regularly, even though they cannot sense light, produce intercellular hormones, or transport water or solutes through intact vessel elements. This substantially narrows down the list possible drivers of dead branch movements. In creosote, we found that dead branch movements consistently tracked relative humidity, with a 1-2 hour lag, at daily and seasonal time scales (Table 4.2). According to our conceptual framework, the fact that dead Branch Position is highly correlated with relative humidity and dead branch movements consistently lag ~2 hours behind changes in relative humidity makes relative humidity a likely candidate for causing subsequent dead branch movements. This suggests that creosote wood has a structure that causes it to passively flex up (skyward) and down (groundward) when exposed to changing humidity. Wood is known to bend in response to changing humidity (Armstrong and Christensen 1961). These deformation patterns differ between species of wood, influencing which species we use as building materials (structural timbers, furniture-grade woods) and wood products (composite boards, paper) (Zhou et al. 1999). However, this kinetic behavior has previously only been associated with cut timber, not wood (live or dead) that is still part of a living plant (Holstov et al. 2015). In our continental survey of branch movements and at our study site, we observed movements in dead branches of living plants, dead woody plants, and fallen logs. Like cut timber, this dead material has more open pores and cracks and less protective bark than live wood. These exposed surfaces can interact with the moisture content and temperature of water, soil, and air, causing different planes of the

wood to passively flex, just like in timber. Further study of branch movements may provide important insights in the mechanical properties of wood from different species, impacting economically important fields such as silviculture, engineering, and material sciences.

We were surprised to find that live creosote branch movements were not related to seasonal patterns of stem water potential but responded primarily to atmospheric water demand (humidity and vapor pressure deficit) (Table 4.2). At least in this species, atmospheric water potential experienced at the stomata seemed to be a more important driver of live branch movements than water potential within the stem. In the absence of leaves, bark, and other living tissues, we would expect live and dead wood on the same plant to behave in more or less similar patterns. Therefore, the differences in the response of these tissues are likely attributable to biotic control over water loss. In creosote, the correlation and time lag between live branches and vapor pressure deficit was more variable than between dead branches and humidity (Figure 4.6, Table 4.2). These patterns also changed seasonally, indicating differing stomatal behavior in different seasons. Other desert shrubs change leaf angles seasonally, optimizing photosynthetic and water conservation capabilities in different environmental regimes (Comstock and Mahall 1985).

4.4.3 Branch Position and plant-environmental feedbacks

Woody plant architecture and non-woody plant movements have repercussions on plant-plant, plant-animal, and plant-environmental feedbacks. In order to investigate how fast branch movements may alter these feedbacks, we compared branch position with soil temperature under the canopies of creosote. We found that soil under creosote canopies was briefly warmed in the early mornings, then shaded and cooled (by more than 3°C in

hot months) for the rest of the day, relative to soils in the intercanopy area. The movement of live, leafy branches was strongly correlated with these cooling effects, suggesting that branch movements may play a role in controlling canopy and soil microclimates in creosote shrublands. Canopy shading has been shown to reduce soil water evaporation in other desert shrubs and trees (Tracol et al. 2011, Royer et al. 2012). Sub-daily branch movements in desert shrubs may enhance canopy shading, increasing soil water retention in the hottest, driest conditions.

Desert shrub canopies play other roles in ecosystem feedbacks. In creosote, branch orientation and leaf inclination reduce heat and water stress to foliar tissues (Ezcurra et al. 1991, 1992). The canopy size and angle of branches play an important role in stemflow, capturing nutrients through dry deposition and funneling them to the base of the plant, localized wind patterns and light penetration into the canopy (Martinez-Meza and Whitford 1996, De Soyza et al. 1997, Whitford et al. 1997, Devakumar et al. 1999, Johnson and Lehmann 2006). *Larrea* species vary in both architecture and branch angles, depending on their latitude and habitat, suggesting that this genus shows plasticity in its architecture in order to adapt to arid conditions. (Ezcurra et al. 1991). In general, desert and cerrado shrubs and saplings with higher branch orientation and straight stems have higher stemflow (Wang et al. 2013, Honda et al. 2015, Levia et al. 2015, Zhang et al. 2017). In addition, branches that have been exposed to different (wind-induced) movements display differing flexibility and oscillations when exposed to wind later in life. So branch flexibility may be adaptive (Sellier and Fourcaud 2005). It is unknown how daily changes in branch position may affect these, and other, biotic and abiotic environmental feedbacks.

4.4.4 Implications and Conclusions

The assumption that woody plants have static architecture permeates many areas of scientific theory and methodology. We encourage fellow scientists to consider diurnal branch movements in future study designs. Anecdotally, we found that differences in branch position within a single day changed total canopy volume and the resulting biomass estimations of creosote individuals by over 20% when using volume: biomass allometric relationships. This diurnal difference in canopy volume could affect the remote-sensed size and position of woody plants measured using drone or TLS techniques.

We recommend further study of branch movements at sites with PhenoCams, especially those we have identified in Table 4.1, by researchers familiar with the environmental context of those sites. We suggest that future studies of branch movements attempt to incorporate a range of individual plant conditions (dead, alive, healthy, sick) and age class as well as environmental conditions to better understand daily and seasonal variation in woody plant architecture. While our continental survey focused on daytime images of plants, previous studies used nighttime TLS pointclouds (Puttonen et al. 2016, Zlinszky et al. 2017). 24-hour observations of branch movements would be ideal. Using automated systems to track branch movements over long study periods may help us understand plant physiology and stress adaptation better in a variety of species and habitats. Beyond simply being an interesting phenomenon, these movements may provide insight into daily changes in stress behavior and environmental interactions previously thought to only change over the course of entire seasons or plant lifetimes.

4.5 Supplemental Appendix C

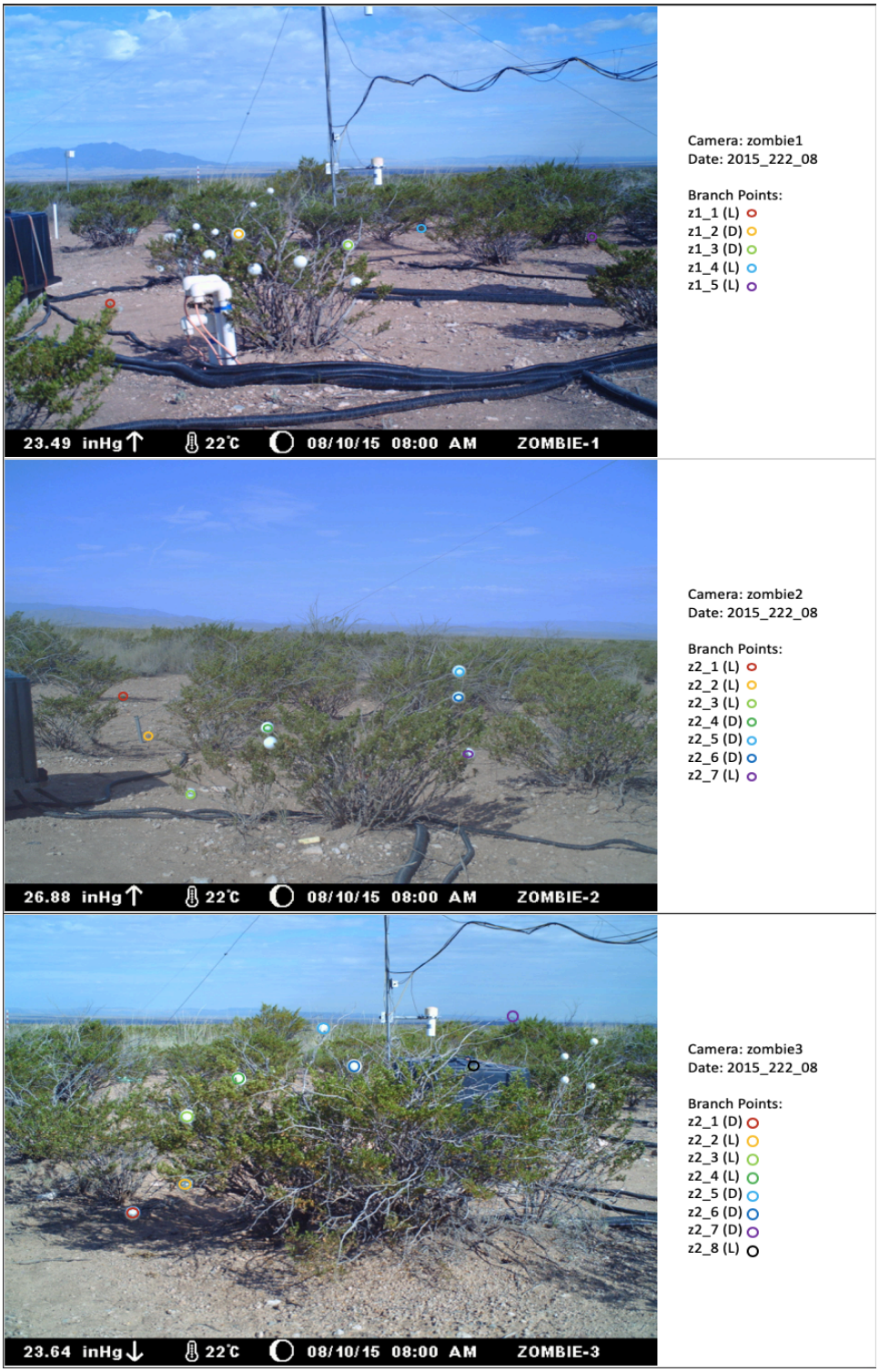

Supplemental Figure C1. All zombie cam scenes, with tracked branches marked with circles. Branch labels indicate whether the branch point was live (L) or dead (D).

Chapter 5

Conclusion

As dryland climates continue to become warmer and more variable, it is crucial to understand how ecosystem functioning will be affected. This functioning is intimately linked to the plant community at a site and the traits of species – especially the dominant species – in that community. In this dissertation, I explored how climate affects dryland plants on multiple scales. In Chapter 2, I compared the relationships between ecosystem functioning and community structure, the seasonal abundance of dominant species, and the daily phenology of common species throughout a decade of climate variation and disturbance recovery. In Chapter 3, I linked the phenological traits of species with the temporal stability of their populations and meteorological associations. Finally, in Chapter 4, I studied the link between hourly branch movements of a widespread desert species, potential abiotic drivers, and possible environmental feedbacks.

In Chapter 2, I found that ecosystem-wide carbon fluxes were more strongly related to the abundance of the dominant species than species diversity in both the desert grassland and creosote shrubland biomes. Our results are similar to others that found that the native, dominant species govern community productivity (Smith and Knapp 2003, Mulder et al. 2004). While we did find that species richness was strongly correlated with ecosystem functioning, this relationship did not translate into a correlation between diversity and ecosystem functioning (Tilman et al. 2001, Maestre et al. 2012). Our results confirm the significance of these foundation species in these biomes. Peters & Yao (2012) found that

the experimental removal of these species resulted in irreversible declines in productivity in these systems. When we compared the annual phenology of common species to carbon fluxes, we found that the dominant species were only most related to fluxes in certain seasons. In the desert grassland, where the dominant species was a C_4 grass, black grama grass phenology was most related to carbon fluxes in the warm, wet monsoon season. In the creosote shrubland, creosote bush (a C_3 shrub) phenology was most related to carbon fluxes in cooler shoulder seasons.

In Chapter 3, we found that the phenological traits of species were related to the temporal stability of their populations. Like previous studies, we found that more conservative – in this case, longer-duration – vegetative growth strategies were employed by species with more stable populations (Lepš et al. 1982, Májeková et al. 2014). We added to these findings by showing that species with more stable populations also produced fruit for more days annually. These phenological traits were associated with enduring a larger range of temperatures and water availability than species that grew and reproduced more quickly. We also found that more stable populations, which had longer average reproductive phenophases, were more likely to fail to produce fruit. This finding demonstrates the trade-off between investment in vegetative growth and reproduction.

In Chapter 4, we documented woody branch movements across a wide range of environments and species. We examined the movements of a desert shrub, creosote bush, in more detail. We found that live branches typically moved a few hours before dead branches moved. We found that live branch movements more closely tracked vapor pressure deficit while dead branch movement were strongly linked to changes in atmospheric humidity. Differences in the timing and potential drivers of live and dead

branch movements were likely related to the fact that leaves on live branches can actively open and close stomata while dead branches have many open pores that are constantly in contact with the open air. We also found that live branch movements had the potential to explain changes in one plant-environmental feedback: soil shading beneath creosote canopies.

References

Adler, P. B., J. HilleRisLambers, P. C. Kyriakidis, Q. Guan, and J. M. Levine. 2006. Climate variability has a stabilizing effect on the coexistence of prairie grasses. Proceedings of the National Academy of Sciences 103:12793–12798.

Ahlström, A., M. R. Raupach, G. Schurgers, B. Smith, A. Arneth, M. Jung, M. Reichstein, J. G. Canadell, P. Friedlingstein, A. K. Jain, E. Kato, B. Poulter, S. Sitch, B. D. Stocker, N. Viovy, Y. P. Wang, A. Wiltshire, S. Zaehle, and N. Zeng. 2015. The dominant role of semi-arid ecosystems in the trend and variability of the land CO2 sink. Science 348:895–899.

Albert, L. P., N. Restrepo-Coupe, M. N. Smith, J. Wu, C. Chavana-Bryant, N. Prohaska, T. C. Taylor, G. A. Martins, P. Ciais, J. Mao, M. A. Arain, W. Li, X. Shi, D. M. Ricciuto, T. E. Huxman, S. M. McMahon, and S. R. Saleska. 2019. Cryptic phenology in plants: Case studies, implications, and recommendations. Global Change Biology 25:3591–3608.

Anderson-Teixeira, K. J., J. P. Delong, A. M. Fox, D. A. Brese, and M. E. Litvak. 2011a. Differential responses of production and respiration to temperature and moisture drive the carbon balance across a climatic gradient in New Mexico. Global Change Biology 17:410–424.

Anderson-Teixeira, K. J., J. P. Delong, A. M. Fox, D. A. Brese, and M. E. Litvak. 2011b. Differential responses of production and respiration to temperature and moisture drive the carbon balance across a climatic gradient in New Mexico. Global Change Biology 17:410–424.

Angert, A. L., T. E. Huxman, G. A. Barron-Gafford, K. L. Gerst, and D. L. Venable. 2007. Linking growth strategies to long-term population dynamics in a guild of desert annuals. Journal of Ecology 95:321–331.

Angert, A. L., T. E. Huxman, P. Chesson, and D. L. Venable. 2009. Functional tradeoffs determine species coexistence via the storage effect. Proceedings of the National Academy of Sciences 106:11641–11645.

Apelt, F., D. Breuer, J. J. Olas, M. G. Annunziata, A. Flis, Z. Nikoloski, F. Kragler, and M. Stitt. 2017. Circadian, Carbon, and Light Control of Expansion Growth and Leaf Movement. Plant Physiology 174:1949–1968.

Armstrong, L. D., and G. N. Christensen. 1961. Influence of Moisture Changes on Deformation of Wood Under Stress | Nature. Nature 191:869–870.

Atamian, H. S., N. M. Creux, E. A. Brown, A. G. Garner, B. K. Blackman, and S. L. Harmer. 2016. Circadian regulation of sunflower heliotropism, floral orientation, and pollinator visits. Science 353:587–590.

Avolio, M. L., E. J. Forrestel, C. C. Chang, K. J. L. Pierre, K. T. Burghardt, and M. D. Smith. 2019. Demystifying dominant species. New Phytologist 223:1106–1126.

Avolio, M. L., S. E. Koerner, K. J. L. Pierre, K. R. Wilcox, G. W. T. Wilson, M. D. Smith, and S. L. Collins. 2014. Changes in plant community composition, not diversity, during a decade of nitrogen and phosphorus additions drive above-ground productivity in a tallgrass prairie. Journal of Ecology 102:1649–1660.

Baer, S. G., J. M. Blair, S. L. Collins, and A. K. Knapp. 2004. Plant Community Responses to Resource Availability and Heterogeneity during Restoration. Oecologia 139:617–629.

Baldocchi, D., E. Falge, L. Gu, R. Olson, D. Hollinger, S. Running, P. Anthoni, C. Bernhofer, K. Davis, R. Evans, J. Fuentes, A. Goldstein, G. Katul, B. Law, X. Lee, Y. Malhi, T. Meyers, W. Munger, W. Oechel, K. T. Paw U, K. Pilegaard, H. P. Schmid, R. Valentini, S. Verma, T. Vesala, K. Wilson, and S. Wofsy. 2001. FLUXNET: A New Tool to Study the Temporal and Spatial Variability of Ecosystem-Scale Carbon Dioxide, Water Vapor, and Energy Flux Densities. Bulletin of the American Meteorological Society 82:2415–2434.

Barber, V. A., G. P. Juday, and B. P. Finney. 2000. Reduced growth of Alaskan white spruce in the twentieth century from temperature-induced drought stress. Nature 405:668–673.

Beatley, J. C. 1974. Phenological Events and Their Environmental Triggers in Mojave Desert Ecosystems. Ecology 55:856–863.

de Bello, F., S. Lavorel, S. Díaz, R. Harrington, J. H. C. Cornelissen, R. D. Bardgett, M. P. Berg, P. Cipriotti, C. K. Feld, D. Hering, P. Martins da Silva, S. G. Potts, L. Sandin, J. P. Sousa, J. Storkey, D. A. Wardle, and P. A. Harrison. 2010. Towards an assessment of multiple ecosystem processes and services via functional traits. Biodiversity and Conservation 19:2873–2893.

Biskup, B., H. Scharr, U. Schurr, and U. Rascher. 2007. A stereo imaging system for measuring structural parameters of plant canopies. Plant, Cell & Environment 30:1299–1308.

Boeck, H. J. D., C. M. H. M. Lemmens, S. Vicca, J. V. den Berge, S. V. Dongen, I. A. Janssens, R. Ceulemans, and I. Nijs. 2007. How do climate warming and species

richness affect CO2 fluxes in experimental grasslands? New Phytologist 175:512–522.

Burnham, K. P., and D. R. Anderson. 2002. Model Selection and Multimodel Inference: A Practical Information-Theoretic Approach. Second edition. Springer-Verlag, New York.

Burrell, A. L., J. P. Evans, and M. G. De Kauwe. 2020. Anthropogenic climate change has driven over 5 million km 2 of drylands towards desertification. Nature Communications 11:3853.

Cárdenas, P., E. Christensen, S. Ernest, D. Lightfoot, R. Schooley, P. Stapp, and J. Rudgers. (n.d.). Declines in rodent abundance and diversity track regional climate variability in North American drylands. Global Change Biology.

Cardinale, B. J., J. E. Duffy, A. Gonzalez, D. U. Hooper, C. Perrings, P. Venail, A. Narwani, G. M. Mace, D. Tilman, D. A. Wardle, A. P. Kinzig, G. C. Daily, M. Loreau, J. B. Grace, A. Larigauderie, D. S. Srivastava, and S. Naeem. 2012. Biodiversity loss and its impact on humanity. Nature 486:59–67.

Cardinale, B., K. Matulich, D. Hooper, J. Byrnes, J. Duffy, L. Gamfeldt, P. Balvanera, M. O'Connor, and A. Gonzalez. 2011. The functional role of producer diversity in ecosystems. American journal of botany 98:572–92.

Catovsky, S., M. A. Bradford, and A. Hector. 2002. Biodiversity and ecosystem productivity: implications for carbon storage. Oikos 97:443–448.

Chesson, P. 2000. Mechanisms of maintenance of species diversity. Annual Review of Ecology and Systematics 31:343–366.

Chesson, P., Gebauer, S. Schwinning, N. Huntly, K. K, M. Ernest, A. Sher, A. Novoplansky, and J. Weltzin. 2004. Resource pulses, species interactions, and diversity maintenance in arid and semi-arid environments. Oecologia 141:236–253.

Chung, Y. A., and J. A. Rudgers. 2016. Plant–soil feedbacks promote negative frequency dependence in the coexistence of two aridland grasses. Proceedings of the Royal Society B: Biological Sciences 283:20160608.

Collins, S. L., J. Belnap, N. B. Grimm, J. A. Rudgers, C. N. Dahm, P. D'Odorico, M. Litvak, D. O. Natvig, D. C. Peters, W. T. Pockman, R. L. Sinsabaugh, and B. O. Wolf. 2014. A Multiscale, Hierarchical Model of Pulse Dynamics in Arid-Land Ecosystems. Annual Review of Ecology, Evolution, and Systematics 45:397–419.

Collins, S. L., A. K. Knapp, J. M. Briggs, J. M. Blair, and E. M. Steinauer. 1998. Modulation of Diversity by Grazing and Mowing in Native Tallgrass Prairie. Science 280:745–747.

Comstock, J. P., and B. E. Mahall. 1985. Drought and changes in leaf orientation for two California chaparral shrubs: Ceanothus megacarpus and Ceanothus crassifolius. Oecologia 65:531–535.

Cook, B. I., and R. Seager. 2013. The response of the North American Monsoon to increased greenhouse gas forcing. Journal of Geophysical Research: Atmospheres 118:1690–1699.

Crimmins, T. M., C. D. Bertelsen, and M. A. Crimmins. 2013. Within-season flowering interruptions are common in the water-limited Sky Islands. International Journal of Biometeorology 58:419–426.

Crimmins, T. M., M. A. Crimmins, and C. D. Bertelsen. 2010. Complex responses to climate drivers in onset of spring flowering across a semi-arid elevation gradient. Journal of Ecology 98:1042–1051.

Crimmins, T. M., M. A. Crimmins, and C. D. Bertelsen. 2011. Onset of summer flowering in a 'Sky Island' is driven by monsoon moisture. New Phytologist 191:468–479.

Darwin, C., and S. F. Darwin. 1880. The Power of Movement in Plants. John Murray, London.

De Soyza, A. G., W. G. Whitford, E. Martinez-Meza, and J. W. Van Zee. 1997. Variation in Creosotebush (Larrea tridentata) Canopy Morphology in Relation to Habitat, Soil Fertility and Associated Annual Plant Communities. The American Midland Naturalist 137:13–26.

Devakumar, A. S., P. Gawai Prakash, M. B. M. Sathik, and J. Jacob. 1999. Drought alters the canopy architecture and micro-climate of Hevea brasiliensis trees. Trees 13:161–167.

Dixon, M. A., and M. T. Tyree. 1984. A new stem hygrometer, corrected for temperature gradients and calibrated against the pressure bomb. Plant, Cell & Environment 7:693–697.

D'Odorico, P., J. D. Fuentes, W. T. Pockman, S. L. Collins, Y. He, J. S. Medeiros, S. Dewekker, and M. E. Litvak. 2010a. Positive feedback between microclimate and shrub encroachment in the northern Chihuahuan desert. Ecosphere.

D'Odorico, P., J. D. Fuentes, W. T. Pockman, S. L. Collins, Y. He, J. S. Medeiros, S. DeWekker, and M. E. Litvak. 2010b. Positive feedback between microclimate and shrub encroachment in the northern Chihuahuan desert. Ecosphere 1:art17.

van Doorn, W. G., and U. van Meeteren. 2003. Flower opening and closure: a review. Journal of Experimental Botany 54:1801–1812.

Duman, T., and K. V. R. Schäfer. 2018. Partitioning net ecosystem carbon exchange of native and invasive plant communities by vegetation cover in an urban tidal wetland in the New Jersey Meadowlands (USA). Ecological Engineering 114:16–24.

Duveneck, M. J., and J. R. Thompson. 2017. Climate change imposes phenological trade-offs on forest net primary productivity. Journal of Geophysical Research: Biogeosciences 122:2298–2313.

Elmendorf, S. C., K. D. Jones, B. I. Cook, J. M. Diez, C. A. F. Enquist, R. A. Hufft, M. O. Jones, S. J. Mazer, A. J. Miller-Rushing, D. J. P. Moore, M. D. Schwartz, and J. F. Weltzin. 2016. The plant phenology monitoring design for the National Ecological Observatory Network.

Elzinga, J. A., A. Atlan, A. Biere, L. Gigord, A. E. Weis, and G. Bernasconi. 2016. Time after time: flowering phenology and biotic interactions. Trends in Ecology & Evolution 22:432–439.

Emery, S. M., and K. L. Gross. 2007. Dominant Species Identity, Not Community Evenness, Regulates Invasion in Experimental Grassland Plant Communities. Ecology 88:954–964.

Ezcurra, E., S. Arizaga, P. L. Valverde, C. Mourelle, and A. Flores-Martínez. 1992. Foliole movement and canopy architecture of Larrea tridentata (DC.) Cov. in Mexican deserts. Oecologia 92:83–89.

Ezcurra, E., C. Montaña, and S. Arizaga. 1991. Architecture, Light Interception, and Distribution of Larrea Species in the Monte Desert, Argentina. Ecology 72:23–34.

Falster, D. S., and M. Westoby. 2003. Leaf size and angle vary widely across species: what consequences for light interception? New Phytologist 158:509–525.

Felton, A. J., and M. D. Smith. 2017. Integrating plant ecological responses to climate extremes from individual to ecosystem levels. Philosophical Transactions of the Royal Society B: Biological Sciences 372:20160142.

Forrest, J., and A. J. Miller-Rushing. 2010. Toward a synthetic understanding of the role of phenology in ecology and evolution. Philosophical Transactions of the Royal Society B: Biological Sciences 365:3101–3112.

Fu, Z., P. C. Stoy, Y. Luo, J. Chen, J. Sun, L. Montagnani, G. Wohlfahrt, A. F. Rahman, S. Rambal, C. Bernhofer, J. Wang, G. Shirkey, and S. Niu. 2017. Climate controls over the net carbon uptake period and amplitude of net ecosystem production in temperate and boreal ecosystems. Agricultural and Forest Meteorology 243:9–18.

Gamon, J. A., and R. W. Pearcy. 1989. Leaf movement, stress avoidance and photosynthesis in Vitis californica. Oecologia 79:475–481.

Garland, T., P. H. Harvey, and A. R. Ives. 1992. Procedures for the Analysis of Comparative Data Using Phylogenetically Independent Contrasts. Systematic Biology 41:18–32.

Gerst, K. L., J. L. Kellermann, C. A. F. Enquist, A. H. Rosemartin, and E. G. Denny. 2016. Estimating the onset of spring from a complex phenology database: trade-offs across geographic scales. International journal of biometeorology.

Gitlin, A. R., C. M. Sthultz, M. A. Bowker, S. Stumpf, K. L. Paxton, K. Kennedy, A. Muñoz, J. K. Bailey, and T. G. Whitham. 2006. Mortality Gradients within and among Dominant Plant Populations as Barometers of Ecosystem Change During Extreme Drought. Conservation Biology 20:1477–1486.

Grantz, K., B. Rajagopalan, M. Clark, and E. Zagona. 2007. Seasonal Shifts in the North American Monsoon. Journal of Climate 20:1923–1935.

Griffith, T. M., and M. A. Watson. 2005. Stress avoidance in a common annual: reproductive timing is important for local adaptation and geographic distribution. Journal of Evolutionary Biology 18:1601–1612.

Grime, J. P. 1998. Benefits of plant diversity to ecosystems: immediate, filter and founder effects. Journal of Ecology 86:902–910.

Grime, J. P., V. K. Brown, K. Thompson, G. J. Masters, S. H. Hillier, I. P. Clarke, A. P. Askew, D. Corker, and J. P. Kielty. 2000. The Response of Two Contrasting Limestone Grasslands to Simulated Climate Change. Science 289:762–765.

Guo, Q., and J. H. Brown. 1996. Temporal Fluctuations and Experimental Effects in Desert Plant Communities. Oecologia 107:568–577.

Gutzler, D. S., and T. O. Robbins. 2010. Climate variability and projected change in the western United States: regional downscaling and drought statistics. Climate Dynamics 37:835–849.

Hallett, L. M., S. K. Jones, A. A. M. MacDonald, M. B. Jones, D. F. B. Flynn, J. Ripplinger, P. Slaughter, C. Gries, and S. L. Collins. 2016. codyn: An r package of community dynamics metrics. Methods in Ecology and Evolution 7:1146–1151.

Han, Q., T. Wang, Y. Jiang, R. Fischer, and C. Li. 2018. Phenological variation decreased carbon uptake in European forests during 1999–2013. Forest Ecology and Management 427:45–51.

Harris, D. J., S. D. Taylor, and E. P. White. 2018. Forecasting biodiversity in breeding birds using best practices. PeerJ 6:e4278.

Harrison, G. W. 1979. Stability under Environmental Stress: Resistance, Resilience, Persistence, and Variability. The American Naturalist 113:659–669.

He, Y., P. D'Odorico, S. F. J. De Wekker, J. D. Fuentes, and M. Litvak. 2010. On the impact of shrub encroachment on microclimate conditions in the northern Chihuahuan desert. Journal of Geophysical Research Atmospheres.

Hector, A., B. Schmid, C. Beierkuhnlein, M. C. Caldeira, M. Diemer, P. G. Dimitrakopoulos, J. A. Finn, H. Freitas, P. S. Giller, J. Good, R. Harris, P. Högberg, K. Huss-Danell, J. Joshi, A. Jumpponen, C. Körner, P. W. Leadley, M. Loreau, A. Minns, C. P. H. Mulder, G. O'Donovan, S. J. Otway, J. S. Pereira, A. Prinz, D. J. Read, M. Scherer-Lorenzen, E.-D. Schulze, A.-S. D. Siamantziouras, E. M. Spehn, A. C. Terry, A. Y. Troumbis, F. I. Woodward, S. Yachi, and J. H. Lawton. 1999. Plant Diversity and Productivity Experiments in European Grasslands. Science 286:1123–1127.

Hendry, A. P., and T. Day. 2005. Population structure attributable to reproductive time: isolation by time and adaptation by time. Molecular Ecology 14:901–916.

Hillebrand, H., B. Blasius, E. T. Borer, J. M. Chase, J. A. Downing, B. K. Eriksson, C. T. Filstrup, W. S. Harpole, D. Hodapp, S. Larsen, A. M. Lewandowska, E. W. Seabloom, D. B. V. de Waal, and A. B. Ryabov. 2018. Biodiversity change is uncoupled from species richness trends: Consequences for conservation and monitoring. Journal of Applied Ecology 55:169–184.

Hirota, M., P. Zhang, S. Gu, H. Shen, T. Kuriyama, Y. Li, and Y. Tang. 2010. Small-scale variation in ecosystem CO2 fluxes in an alpine meadow depends on plant biomass and species richness. Journal of Plant Research 123:531–541.

Holstov, A., B. Bridgens, and G. Farmer. 2015. Hygromorphic materials for sustainable responsive architecture. Construction and Building Materials 98:570–582.

Honda, E. A., A. H. Mendonça, and G. Durigan. 2015. Factors affecting the stemflow of trees in the Brazilian Cerrado. Ecohydrology 8:1351–1362.

Hooper, D. U., F. S. Chapin III, J. J. Ewel, A. Hector, P. Inchausti, S. Lavorel, J. H. Lawton, D. M. Lodge, M. Loreau, S. Naeem, B. Schmid, H. Setälä, A. J. Symstad, J. Vandermeer, and D. A. Wardle. 2016. Effects of biodiversity on ecosystem functioning: a consensus of current knowledge. Ecological Monographs:3–35.

Huang, J., M. Ji, Y. Xie, S. Wang, Y. He, and J. Ran. 2015. Global semi-arid climate change over last 60 years. Climate Dynamics 46:1131–1150.

Huang, L., W. Xue, and T. Herben. 2019. Temporal niche differentiation among species changes with habitat productivity and light conditions. Journal of Vegetation Science 30:438–447.

Huenneke, L. F., D. Clason, and E. Muldavin. 2001. Spatial heterogeneity in Chihuahuan Desert vegetation: implications for sampling methods in semi-arid ecosystems. Journal of Arid Environments 47:257–270.

Hufkens, K., M. Friedl, O. Sonnentag, B. H. Braswell, T. Milliman, and A. D. Richardson. 2012. Linking near-surface and satellite remote sensing measurements of deciduous broadleaf forest phenology. Remote Sensing of Environment 117:307–321.

Hulshof, C. M., J. C. Stegen, N. G. Swenson, C. A. F. Enquist, and B. J. Enquist. 2012. Interannual variability of growth and reproduction in Bursera simaruba: the role of allometry and resource variability. Ecology 93:180–190.

Ibáñez, I., E. S. Gornish, L. Buckley, D. M. Debinski, J. Hellmann, B. Helmuth, J. HilleRisLambers, A. M. Latimer, A. J. Miller-Rushing, and M. Uriarte. 2013. Moving forward in global-change ecology: capitalizing on natural variability. Ecology and Evolution 3:170–181.

Iida, S., T. Tanaka, and M. Sugita. 2005. Change of interception process due to the succession from Japanese red pine to evergreen oak. Journal of Hydrology 315:154–166.

Inouye, B. D., J. Ehrlén, and N. Underwood. 2019. Phenology as a process rather than an event: from individual reaction norms to community metrics. Ecological Monographs 89:e01352.

Inouye, D. W. 2008. Effects of Climate Change on Phenology, Frost Damage, and Floral Abundance of Montane Wildflowers. Ecology 89:353–362.

IPCC, 2013. 2013. Climate Change 2013: The Physical Science Basis. Contribution of Working Group I to the Fifth Assessment Report of the Intergovernmental Panel on Climate Change. Page (T. F. Stocker, D. Qin, G.-K. Plattner, M. Tignor, S. K. Allen, J. Boschung, A. Nauels, Y. Xia, V. Bex, and P. M. Midgley, Eds.). Cambridge University Press, Cambridge, United Kingdom and New York, NY, USA.

Jiguet, F., A.-S. Gadot, R. Julliard, S. E. Newson, and D. Couvet. 2007. Climate envelope, life history traits and the resilience of birds facing global change. Global Change Biology 13:1672–1684.

Johnson, M. S., and J. Lehmann. 2006. Double-funneling of trees: Stemflow and root-induced preferential flow.

Kahmen, A., J. Perner, V. Audorff, W. Weisser, and N. Buchmann. 2005. Effects of plant diversity, community composition and environmental parameters on productivity in montane European grasslands. Oecologia 142:606–615.

Kao, W.-Y., and I. N. Forseth. 1992. Dirunal leaf movement, chlorophyll fluorescence and carbon assimilation in soybean grown under different nitrogen and water availabilities. Plant, Cell & Environment 15:703–710.

Karban, R. 2008. Plant behaviour and communication. Ecology Letters 11:727–739.

Kazenel, M. R., S. N. Kivlin, D. L. Taylor, J. S. Lynn, and J. A. Rudgers. 2019. Altitudinal gradients fail to predict fungal symbiont responses to warming. Ecology 100:e02740.

Keller, M., D. S. Schimel, W. W. Hargrove, and F. M. Hoffman. 2008. A continental strategy for the National Ecological Observatory Network. Frontiers in Ecology and the Environment 6:282–284.

Kelly, D., and V. L. Sork. 2002. Mast Seeding in Perennial Plants: Why, How, Where? Annual Review of Ecology and Systematics 33:427–447.

Kindvall, O. 1996. Habitat Heterogeneity and Survival in a Bush Cricket Metapopulation. Ecology 77:207–214.

Kominoski, J. S., E. E. Gaiser, and S. G. Baer. 2018. Advancing Theories of Ecosystem Development through Long-Term Ecological Research. BioScience 68:554–562.

Ladwig, L. M., S. L. Collins, D. J. Krofcheck, and W. T. Pockman. 2019. Minimal mortality and rapid recovery of the dominant shrub Larrea tridentata following an extreme cold event in the northern Chihuahuan Desert. Journal of Vegetation Science 30:963–972.

Laganière, J., X. Cavard, B. W. Brassard, D. Paré, Y. Bergeron, and H. Y. H. Chen. 2015. The influence of boreal tree species mixtures on ecosystem carbon storage and fluxes. Forest Ecology and Management 354:119–129.

Lal, R. 2003. Carbon Sequestration in Dryland Ecosystems. Environmental Management 33:528–544.

Lasky, J. R., M. Uriarte, and R. Muscarella. 2016. Synchrony, compensatory dynamics, and the functional trait basis of phenological diversity in a tropical dry forest tree community: effects of rainfall seasonality. Environmental Research Letters 11:115003.

Lasslop, G., M. Migliavacca, G. Bohrer, M. Reichstein, M. Bahn, A. Ibrom, C. Jacobs, P. Kolari, D. Papale, T. Vesala, G. Wohlfahrt, and A. Cescatti. 2012. On the choice of the driving temperature for eddy-covariance carbon dioxide flux partitioning. Biogeosciences 9:5243–5259.

Lavorel, S., and E. Garnier. 2002. Predicting changes in community composition and ecosystem functioning from plant traits: revisiting the Holy Grail. Functional Ecology 16:545–556.

Lepš, J., J. Osbornová-Kosinová, and M. Rejmánek. 1982. Community Stability, Complexity and Species Life History Strategies. Vegetatio 50:53–63.

Levia, D. F., B. Michalzik, K. Näthe, S. Bischoff, S. Richter, and D. R. Legates. 2015. Differential stemflow yield from European beech saplings: the role of individual canopy structure metrics. Hydrological Processes 29:43–51.

Ludlow, M. M., and O. Björkman. 1984. Paraheliotropic leaf movement in Siratro as a protective mechanism against drought-induced damage to primary photosynthetic reactions: damage by excessive light and heat. Planta 161:505–518.

Lyons, K. G., and M. W. Schwartz. 2001. Rare species loss alters ecosystem function – invasion resistance. Ecology Letters 4:358–365.

Ma, F., F. Zhang, Q. Quan, B. Song, J. Wang, Q. Zhou, and S. Niu. 2020. Common Species Stability and Species Asynchrony Rather than Richness Determine Ecosystem Stability Under Nitrogen Enrichment. Ecosystems.

MacGillivray, C. W., and J. P. (NERC U. of C. P. E. Grime. 1995. Testing predictions of the resistance and resilience of vegetation subjected to extreme events. Functional Ecology (United Kingdom).

Maestre, F. T., J. L. Quero, N. J. Gotelli, A. Escudero, V. Ochoa, M. Delgado-Baquerizo, M. García-Gómez, M. A. Bowker, S. Soliveres, C. Escolar, P. García-Palacios, M. Berdugo, E. Valencia, B. Gozalo, A. Gallardo, L. Aguilera, T. Arredondo, J. Blones, B. Boeken, D. Bran, A. A. Conceição, O. Cabrera, M. Chaieb, M. Derak, D. J. Eldridge, C. I. Espinosa, A. Florentino, J. Gaitán, M. G. Gatica, W. Ghiloufi, S. Gómez-González, J. R. Gutiérrez, R. M. Hernández, X. Huang, E. Huber-Sannwald, M. Jankju, M. Miriti, J. Monerris, R. L. Mau, E. Morici, K. Naseri, A. Ospina, V. Polo, A. Prina, E. Pucheta, D. A. Ramírez-Collantes, R. Romão, M. Tighe, C. Torres-Díaz, J. Val, J. P. Veiga, D. Wang, and E. Zaady. 2012. Plant Species Richness and Ecosystem Multifunctionality in Global Drylands. Science 335:214–218.

Májeková, M., F. de Bello, J. Doležal, and J. Lepš. 2014. Plant functional traits as determinants of population stability. Ecology 95:2369–2374.

Martinez-Meza, E., and W. G. Whitford. 1996. Stemflow, throughfall and channelization of stemflow by roots in three Chihuahuan desert shrubs. Journal of Arid Environments 32:271–287.

Massman, W. J. 2000. A simple method for estimating frequency response corrections for eddy covariance systems. Agricultural and Forest Meteorology 104:185–198.

Maurer, G. E., A. J. Hallmark, R. F. Brown, O. E. Sala, and S. L. Collins. 2020. Sensitivity of primary production to precipitation across the United States. Ecology Letters 23:527–536.

Medeiros, J. S., and W. T. Pockman. 2011. Drought increases freezing tolerance of both leaves and xylem of Larrea tridentata. Plant, Cell & Environment 34:43–51.

Melo-Merino, S. M., H. Reyes-Bonilla, and A. Lira-Noriega. 2020. Ecological niche models and species distribution models in marine environments: A literature review and spatial analysis of evidence. Ecological Modelling 415:108837.

Migliavacca, M., M. Galvagno, E. Cremonese, M. Rossini, M. Meroni, O. Sonnentag, S. Cogliati, G. Manca, F. Diotri, L. Busetto, A. Cescatti, R. Colombo, F. Fava, U. Morra di Cella, E. Pari, C. Siniscalco, and A. D. Richardson. 2011. Using digital repeat photography and eddy covariance data to model grassland phenology and photosynthetic CO2 uptake. Agricultural and Forest Meteorology 151:1325–1337.

Monson, R. K., M. R. Prater, J. Hu, S. P. Burns, J. P. Sparks, K. L. Sparks, and L. E. Scott-Denton. 2010. Tree species effects on ecosystem water-use efficiency in a high-elevation, subalpine forest. Oecologia 162:491–504.

Morin, X., M. J. Lechowicz, C. Augspurger, J. O'keefe, D. Viner, and I. Chuine. 2009. Leaf phenology in 22 North American tree species during the 21st century. Global Change Biology 15:961–975.

Moussus, J.-P., J. Clavel, F. Jiguet, and R. Julliard. 2011. Which are the phenologically flexible species? A case study with common passerine birds. Oikos 120:991–998.

Muldavin, E. H., D. I. Moore, S. L. Collins, K. R. Wetherill, and D. C. Lightfoot. 2008. Aboveground net primary production dynamics in a northern Chihuahuan Desert ecosystem. Oecologia 155:123–132.

Mulder, C. P. H., E. Bazeley-White, P. G. Dimitrakopoulos, A. Hector, M. Scherer-Lorenzen, and B. Schmid. 2004. Species evenness and productivity in experimental plant communities. Oikos 107:50–63.

Nichols, M. H., J. C. Steven, R. Sargent, P. Dille, and J. Schapiro. 2013. Very-high-resolution time-lapse photography for plant and ecosystems research. Applications in Plant Sciences 1:1300033.

Niinemets, Ü. 2010. A review of light interception in plant stands from leaf to canopy in different plant functional types and in species with varying shade tolerance. Ecological Research 25:693–714.

Nilsen, E. T. 1987. Influence of Water Relations and Temperature on Leaf Movements of Rhododendron Species. Plant Physiology 83:607–612.

Nilsen, E. T. 1991. The relationship between freezing tolerance and thermotropic leaf movement in five Rhododendron species. Oecologia 87:63–71.

Norman, J. M., and G. S. Campbell. 1989. Canopy structure. Pages 301–325 *in* R. W. Pearcy, J. R. Ehleringer, H. A. Mooney, and P. W. Rundel, editors. Plant Physiological Ecology: Field methods and instrumentation. Springer Netherlands, Dordrecht.

Novick, K. A., J. A. Biederman, A. R. Desai, M. E. Litvak, D. J. P. Moore, R. L. Scott, and M. S. Torn. 2018. The AmeriFlux network: A coalition of the willing. Agricultural and Forest Meteorology 249:444–456.

Noy-Meir, I. 1973. Desert ecosystems: environment and producers. Annual review of ecology and systematics.

Ogle, K., J. J. Barber, G. A. Barron-Gafford, L. P. Bentley, J. M. Young, T. E. Huxman, M. E. Loik, and D. T. Tissue. 2015. Quantifying ecological memory in plant and ecosystem processes. Ecology Letters 18:221–235.

Orwin, K. H., S. M. Buckland, D. Johnson, B. L. Turner, S. Smart, S. Oakley, and R. D. Bardgett. 2010. Linkages of plant traits to soil properties and the functioning of temperate grassland. Journal of Ecology 98:1074–1083.

Orwin, K. H., N. Ostle, A. Wilby, and R. D. Bardgett. 2014. Effects of species evenness and dominant species identity on multiple ecosystem functions in model grassland communities. Oecologia 174:979–992.

Ovaskainen, O., S. Skorokhodova, M. Yakovleva, A. Sukhov, A. Kutenkov, N. Kutenkova, A. Shcherbakov, E. Meyke, and M. del M. Delgado. 2013. Community-level phenological response to climate change. Proceedings of the National Academy of Sciences 110:13434–13439.

Pagel, M. 1999. Inferring the historical patterns of biological evolution. Nature 401:877–884.

Paradis, E., and K. Schliep. 2019. ape 5.0: an environment for modern phylogenetics and evolutionary analyses in R. Bioinformatics 35:526–528.

Parmesan, C., and G. Yohe. 2003. A globally coherent fingerprint of climate change impacts across natural systems. Nature 421:37–42.

Pau, S., E. M. Wolkovich, B. I. Cook, T. J. Davies, N. J. B. Kraft, K. Bolmgren, J. L. Betancourt, and E. E. Cleland. 2011. Predicting phenology by integrating ecology, evolution and climate science. Global Change Biology 17:3633–3643.

Peñuelas, J., I. Filella, X. Zhang, L. Llorens, R. Ogaya, F. Lloret, P. Comas, M. Estiarte, and J. Terradas. 2004. Complex spatiotemporal phenological shifts as a response to rainfall changes. New Phytologist 161:837–846.

Petach, A. R., M. Toomey, D. M. Aubrecht, and A. D. Richardson. 2014. Monitoring vegetation phenology using an infrared-enabled security camera. Agricultural and Forest Meteorology 195–196:143–151.

Peters, D. P. C., and J. Yao. 2012. Long-term experimental loss of foundation species: consequences for dynamics at ecotones across heterogeneous landscapes. Ecosphere 3:art27.

Petrie, M. D., S. L. Collins, D. S. Gutzler, and D. M. Moore. 2014. Regional trends and local variability in monsoon precipitation in the northern Chihuahuan Desert, USA. Journal of Arid Environments 103:63–70.

Petrie, M. D., S. L. Collins, A. M. Swann, P. L. Ford, and M. E. Litvak. 2015a. Grassland to shrubland state transitions enhance carbon sequestration in the northern Chihuahuan Desert. Global Change Biology 21:1226–1235.

Petrie, M. D., S. L. Collins, A. M. Swann, P. L. Ford, and M. E. Litvak. 2015b. Grassland to shrubland state transitions enhance carbon sequestration in the northern Chihuahuan Desert. Global Change Biology.

Pilson, D. 2000. Herbivory and natural selection on flowering phenology in wild sunflower, Helianthus annuus. Oecologia 122:72–82.

Pockman, W. T., and J. S. Sperry. 1997. Freezing-Induced Xylem Cavitation and the Northern Limit of Larrea tridentata. Oecologia 109:19–27.

Polgar, C. A., and R. B. Primack. 2011. Leaf-out phenology of temperate woody plants: from trees to ecosystems. New Phytologist 191:926–941.

Polley, H. W., F. I. Isbell, and B. J. Wilsey. 2013. Plant functional traits improve diversity-based predictions of temporal stability of grassland productivity. Oikos 122:1275–1282.

Prăvălie, R. 2016. Drylands extent and environmental issues. A global approach. Earth-Science Reviews 161:259–278.

Primack, R. B., and A. J. Miller-Rushing. 2011. Broadening the study of phenology and climate change. New Phytologist 191:307–309.

Puttonen, E., C. Briese, G. Mandlburger, M. Wieser, M. Pfennigbauer, A. Zlinszky, and N. Pfeifer. 2016. Quantification of Overnight Movement of Birch (Betula pendula) Branches and Foliage with Short Interval Terrestrial Laser Scanning. Frontiers in Plant Science 7.

R Core Team. 2020. R: A Language and Environment for Statistical Computing. R Foundation for Statistical Computing, Vienna, Austria.

Revell, L. 2012. phytools: An R package for phylogenetic comparative biology (and other things). Methods in Ecology and Evolution 3:217–223.

Reynolds, J. F., D. M. S. Smith, E. F. Lambin, B. L. Turner, M. Mortimore, S. P. J. Batterbury, T. E. Downing, H. Dowlatabadi, R. J. Fernández, J. E. Herrick, E. Huber-Sannwald, H. Jiang, R. Leemans, T. Lynam, F. T. Maestre, M. Ayarza, and B. Walker. 2007. Global Desertification: Building a Science for Dryland Development. Science 316:847–851.

Richardson, A. D., T. Andy Black, P. Ciais, N. Delbart, M. A. Friedl, N. Gobron, D. Y. Hollinger, W. L. Kutsch, B. Longdoz, S. Luyssaert, M. Migliavacca, L. Montagnani, J. William Munger, E. Moors, S. Piao, C. Rebmann, M. Reichstein,

N. Saigusa, E. Tomelleri, R. Vargas, and A. Varlagin. 2010. Influence of spring and autumn phenological transitions on forest ecosystem productivity. Philosophical Transactions of the Royal Society B: Biological Sciences 365:3227–3246.

Richardson, A. D., K. Hufkens, T. Milliman, D. M. Aubrecht, M. E. Furze, B. Seyednasrollah, M. B. Krassovski, J. M. Latimer, W. R. Nettles, R. R. Heiderman, J. M. Warren, and P. J. Hanson. 2018. Ecosystem warming extends vegetation activity but heightens vulnerability to cold temperatures. Nature 560:368–371.

Richardson, A. D., J. P. Jenkins, B. H. Braswell, D. Y. Hollinger, S. V. Ollinger, and M.-L. Smith. 2007. Use of digital webcam images to track spring green-up in a deciduous broadleaf forest. Oecologia 152:323–334.

Ridolfi, L., P. D'Odorico, and F. Laio. 2011. Noise-Induced Phenomena in the Environmental Sciences. Cambridge University Press.

Royer, P. D., D. D. Breshears, C. B. Zou, J. C. Villegas, N. S. Cobb, and S. A. Kurc. 2012. Density-Dependent Ecohydrological Effects of Piñon–Juniper Woody Canopy Cover on Soil Microclimate and Potential Soil Evaporation. Rangeland Ecology and Management 65:11–20.

Rudgers, J. A., Y. A. Chung, G. E. Maurer, D. I. Moore, E. H. Muldavin, M. E. Litvak, and S. L. Collins. 2018. Climate sensitivity functions and net primary production: A framework for incorporating climate mean and variability. Ecology 99:576–582.

Rudgers, J. A., A. Hallmark, S. R. Baker, L. Baur, K. M. Hall, M. E. Litvak, E. H. Muldavin, W. T. Pockman, and K. D. Whitney. 2019. Sensitivity of dryland plant allometry to climate. Functional Ecology 33:2290–2303.

Rutledge, S., A. M. Wall, P. L. Mudge, B. Troughton, D. I. Campbell, J. Pronger, C. Joshi, and L. A. Schipper. 2017. The carbon balance of temperate grasslands part I: The impact of increased species diversity. Agriculture, Ecosystems & Environment 239:310–323.

Sagar, R., G. Y. Li, J. S. Singh, and S. Wan. 2019. Carbon fluxes and species diversity in grazed and fenced typical steppe grassland of Inner Mongolia, China. Journal of Plant Ecology 12:10–22.

Saiz, H., Y. L. Bagousse-Pinguet, N. Gross, and F. T. Maestre. 2019. Intransitivity increases plant functional diversity by limiting dominance in drylands worldwide. Journal of Ecology 107:240–252.

Sala, O. E., L. A. Gherardi, L. Reichmann, E. Jobbágy, and D. Peters. 2012. Legacies of precipitation fluctuations on primary production: theory and data synthesis. Philosophical Transactions of the Royal Society B: Biological Sciences 367:3135–3144.

Sauer, J. R., and W. A. Link. 2002. Hierarchical Modeling of Population Stability and Species Group Attributes from Survey Data. Ecology 83:1743–1751.

Sellier, D., and T. Fourcaud. 2005. A mechanical analysis of the relationship between free oscillations of Pinus pinaster Ait. saplings and their aerial architecture. Journal of Experimental Botany 56:1563–1573.

Seyednasrollah, B., A. M. Young, K. Hufkens, T. Milliman, M. A. Friedl, S. Frolking, and A. D. Richardson. 2019. Tracking vegetation phenology across diverse biomes using Version 2.0 of the PhenoCam Dataset. Scientific Data 6:222.

Silletti, A., and A. Knapp. 2002. Long-Term Responses of the Grassland Co-Dominants Andropogon gerardii and Sorghastrum nutans to Changes in Climate and Management. Plant Ecology 163:15–22.

Silva, P. F. da, J. R. de S. Lima, A. C. D. Antonino, R. Souza, E. S. de Souza, J. R. I. Silva, and E. M. Alves. 2017. Seasonal patterns of carbon dioxide, water and energy fluxes over the Caatinga and grassland in the semi-arid region of Brazil. Journal of Arid Environments 147:71–82.

Silvertown, J., Y. Araya, and D. Gowing. 2015. Hydrological niches in terrestrial plant communities: a review. Journal of Ecology 103:93–108.

Smith, A. P. 1974. Bud Temperature in Relation to Nyctinastic Leaf Movement in an Andean Giant Rosette Plant. Biotropica 6:263–266.

Smith, B., and J. B. Wilson. 1996. A Consumer's Guide to Evenness Indices. Oikos 76:70–82.

Smith, M. D., and A. K. Knapp. 2003. Dominant species maintain ecosystem function with non-random species loss. Ecology Letters 6:509–517.

Sonkoly, J., A. Kelemen, O. Valkó, B. Deák, R. Kiss, K. Tóth, T. Miglécz, B. Tóthmérész, and P. Török. 2019. Both mass ratio effects and community diversity drive biomass production in a grassland experiment. Scientific Reports 9:1848.

Stearns, S. C. 1992. The Evolution of Life Histories. OUP Oxford.

Su, F., Y. Wei, F. Wang, J. Guo, J. Zhang, Y. Wang, H. Guo, and S. Hu. 2019. Sensitivity of plant species to warming and altered precipitation dominates the community productivity in a semiarid grassland on the Loess Plateau. Ecology and Evolution 9:7628–7638.

Taylor, J. A., and J. Lloyd. 1992. Sources and Sinks of Atmospheric CO2. Australian Journal of Botany 40:407–418.

Thackeray, S. J., P. A. Henrys, D. Hemming, J. R. Bell, M. S. Botham, S. Burthe, P. Helaouet, D. G. Johns, I. D. Jones, D. I. Leech, E. B. Mackay, D. Massimino, S. Atkinson, P. J. Bacon, T. M. Brereton, L. Carvalho, T. H. Clutton-Brock, C. Duck, M. Edwards, J. M. Elliott, S. J. G. Hall, R. Harrington, J. W. Pearce-Higgins, T. T. Høye, L. E. B. Kruuk, J. M. Pemberton, T. H. Sparks, P. M. Thompson, I. White, I. J. Winfield, and S. Wanless. 2016. Phenological sensitivity to climate across taxa and trophic levels. Nature 535:241–245.

The MathWorks Inc. 2019. MATLAB. Natick, Massachusetts.

Thomson, J. D. 2010. Flowering phenology, fruiting success and progressive deterioration of pollination in an early-flowering geophyte. Philosophical Transactions of the Royal Society B: Biological Sciences 365:3187–3199.

Tilman, D., P. B. Reich, J. Knops, D. Wedin, T. Mielke, and C. Lehman. 2001. Diversity and Productivity in a Long-Term Grassland Experiment. Science 294:843–845.

Toomey, M., M. A. Friedl, S. Frolking, K. Hufkens, S. Klosterman, O. Sonnentag, D. D. Baldocchi, C. J. Bernacchi, S. C. Biraud, G. Bohrer, E. Brzostek, S. P. Burns, C. Coursolle, D. Y. Hollinger, H. A. Margolis, H. McCaughey, R. K. Monson, J. W. Munger, S. Pallardy, R. P. Phillips, M. S. Torn, S. Wharton, M. Zeri, and A. D.

Richardson. 2015. Greenness indices from digital cameras predict the timing and seasonal dynamics of canopy-scale photosynthesis. Ecological Applications 25:99–115.

Tracol, Y., J. R. Gutiérrez, and F. A. Squeo. 2011. Plant Area Index and microclimate underneath shrub species from a Chilean semiarid community. Journal of Arid Environments 75:1–6.

USDA, NRCS. 2020. The PLANTS Database. National Plant Data Team, Greensboro, NC 27401-4901 USA.

Valladares, F., and F. I. Pugnaire. 1999. Tradeoffs Between Irradiance Capture and Avoidance in Semi-arid Environments Assessed with a Crown Architecture Model. Annals of Botany 83:459–469.

Venable, D. L. 2007. Bet Hedging in a Guild of Desert Annuals. Ecology 88:1086–1090.

Venable, D. L., and S. Kimball. 2012. Population and community dynamics in variable environments: The desert annual system. Temporal Dynamics and Ecological Process:140–164.

Visser, M. E., and L. J. M. Holleman. 2001. Warmer springs disrupt the synchrony of oak and winter moth phenology. Proceedings of the Royal Society of London. Series B: Biological Sciences 268:289–294.

Wang, R., J. A. Gamon, C. A. Emmerton, H. Li, E. Nestola, G. Z. Pastorello, and O. Menzer. 2016. Integrated Analysis of Productivity and Biodiversity in a Southern Alberta Prairie. Remote Sensing 8:214.

Wang, X., Y. Zhang, Z. Wang, Y. Pan, R. Hu, X. Li, and H. Zhang. 2013. Influence of shrub canopy morphology and rainfall characteristics on stemflow within a

revegetated sand dune in the Tengger Desert, NW China. Hydrological Processes 27:1501–1509.

Webb, E. K., G. I. Pearman, and R. Leuning. 1980. Correction of flux measurements for density effects due to heat and water vapour transfer. Quarterly Journal of the Royal Meteorological Society 106:85–100.

White, M. A., and R. R. Nemani. 2003. Canopy duration has little influence on annual carbon storage in the deciduous broad leaf forest. Global Change Biology 9:967–972.

Whitford, W., J. Anderson, and P. Rice. 1997. Stemflow contribution to the 'fertile island' effect in creosotebush,Larrea tridentata. Journal of Arid Environments 35:451–457.

Whittaker, R. H. 1965. Dominance and Diversity in Land Plant Communities: Numerical relations of species express the importance of competition in community function and evolution. Science 147:250–260.

Wilcox, K. R., J. M. Blair, M. D. Smith, and A. K. Knapp. 2016. Does ecosystem sensitivity to precipitation at the site-level conform to regional-scale predictions? Ecology 97:561–568.

Winfree, R., J. W. Fox, N. M. Williams, J. R. Reilly, and D. P. Cariveau. 2015. Abundance of common species, not species richness, drives delivery of a real-world ecosystem service. Ecology Letters 18:626–635.

Wolkovich, E. M., B. I. Cook, J. M. Allen, T. M. Crimmins, J. L. Betancourt, S. E. Travers, S. Pau, J. Regetz, T. J. Davies, N. J. B. Kraft, T. R. Ault, K. Bolmgren, S. J. Mazer, G. J. McCabe, B. J. McGill, C. Parmesan, N. Salamin, M. D.

Schwartz, and E. E. Cleland. 2012. Warming experiments underpredict plant phenological responses to climate change. Nature 485:494–497.

Xu, F., W. Guo, R. Wang, W. Xu, N. Du, and Y. Wang. 2009. Leaf movement and photosynthetic plasticity of black locust (Robinia pseudoacacia) alleviate stress under different light and water conditions. Acta Physiologiae Plantarum 31:553–563.

Yan, D., R. L. Scott, D. J. P. Moore, J. A. Biederman, and W. K. Smith. 2019. Understanding the relationship between vegetation greenness and productivity across dryland ecosystems through the integration of PhenoCam, satellite, and eddy covariance data. Remote Sensing of Environment 223:50–62.

Zhang, Y., M. Loreau, X. Lü, N. He, G. Zhang, and X. Han. 2016. Nitrogen enrichment weakens ecosystem stability through decreased species asynchrony and population stability in a temperate grassland. Global Change Biology 22:1445–1455.

Zhang, Y., X. Wang, R. Hu, and Y. Pan. 2017. Stemflow volume per unit rainfall as a good variable to determine the relationship between stemflow amount and morphological metrics of shrubs. Journal of Arid Environments 141:1–6.

Zhou, Y., M. Fushitani, T. Kubo, and M. Ozawa. 1999. Bending creep behavior of wood under cyclic moisture changes. Journal of Wood Science 45:113–119.

Zlinszky, A., B. Molnár, and A. S. Barfod. 2017. Not All Trees Sleep the Same—High Temporal Resolution Terrestrial Laser Scanning Shows Differences in Nocturnal Plant Movement. Frontiers in Plant Science 8.